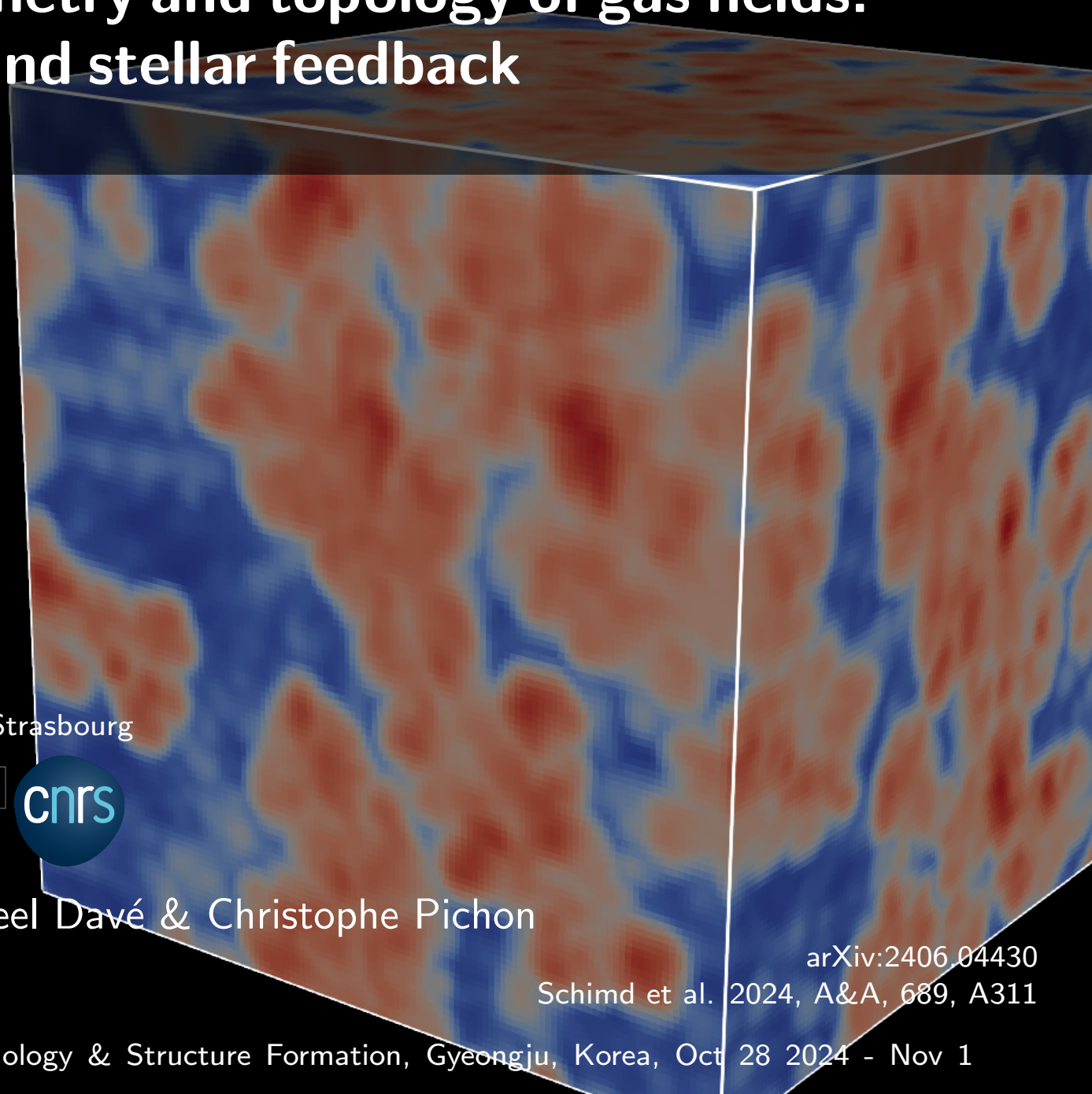
Large-scale geometry and topology of gas fields: Effects of AGN and stellar feedback



Katarina Kraljic

Observatoire astronomique de Strasbourg

w/ Carlo Schimd, Romeel Davé & Christophe Pichon

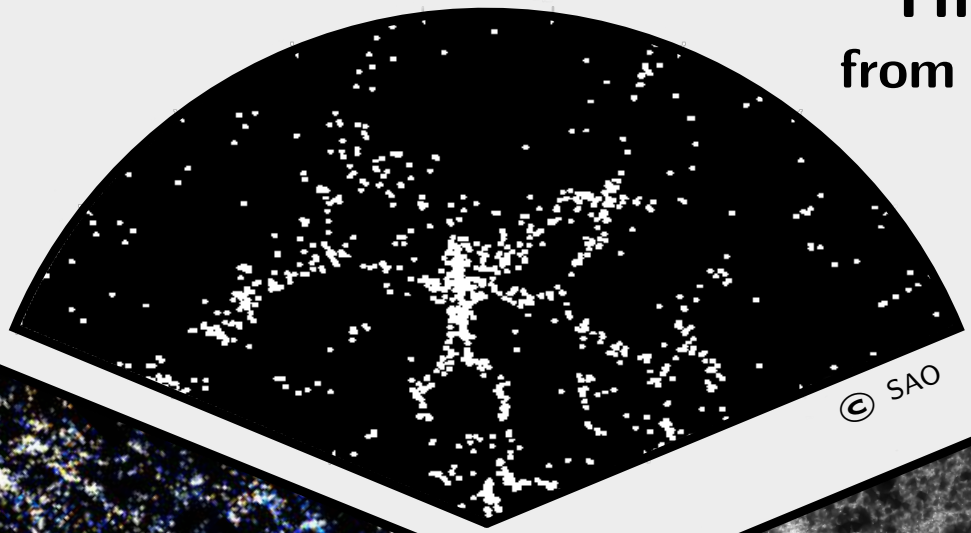
arXiv:2406.04430

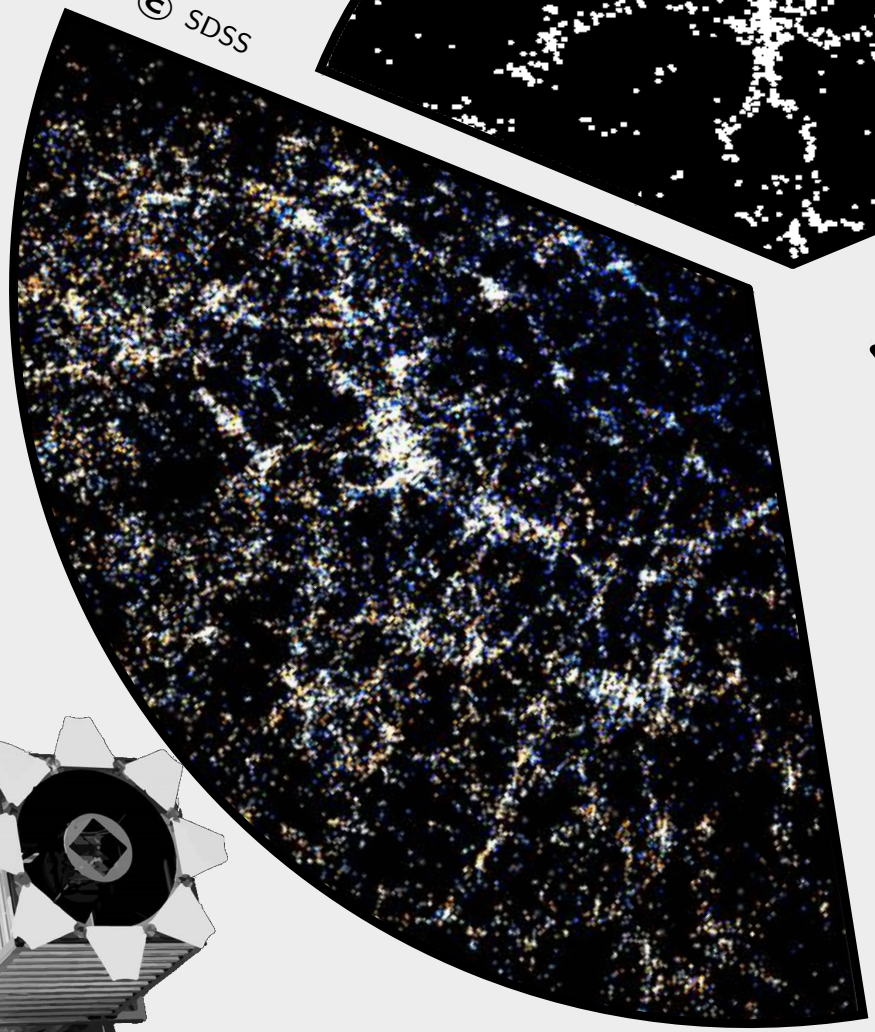
Schimd et al. 2024, A&A, 689, A311

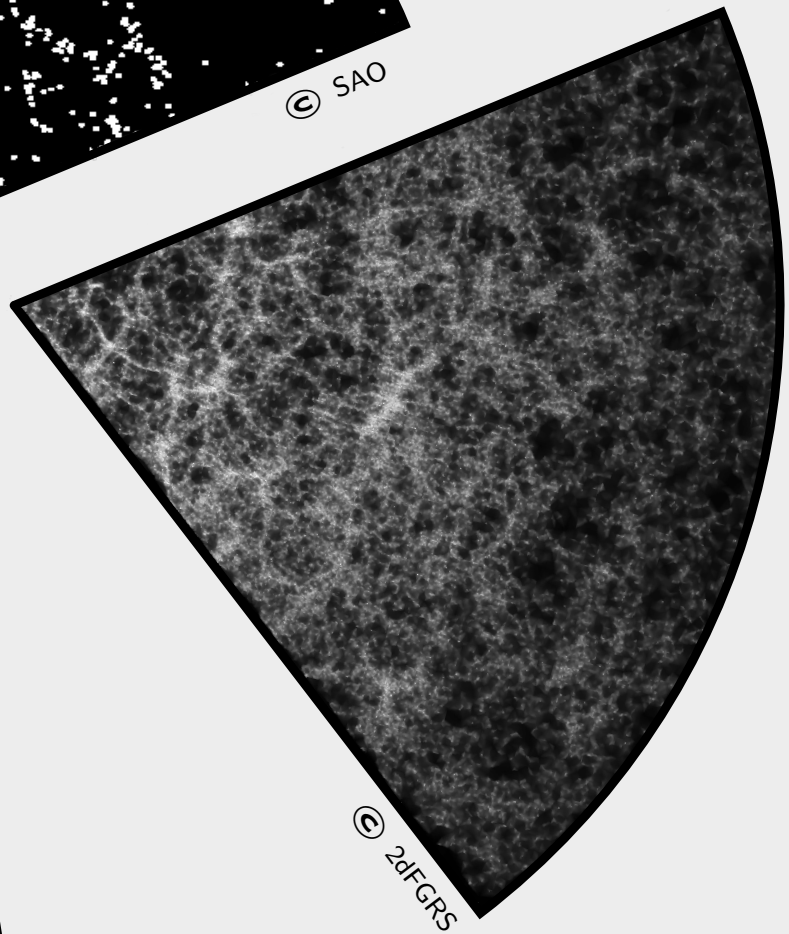
11th KIAS Workshop on Cosmology & Structure Formation, Gyeongju, Korea, Oct 28 2024 - Nov 1

The Cosmic web
from observations . . .

de Lapparent et al. 1986
Colless et al. 2003
Adelman-McCarthy et al. 2008





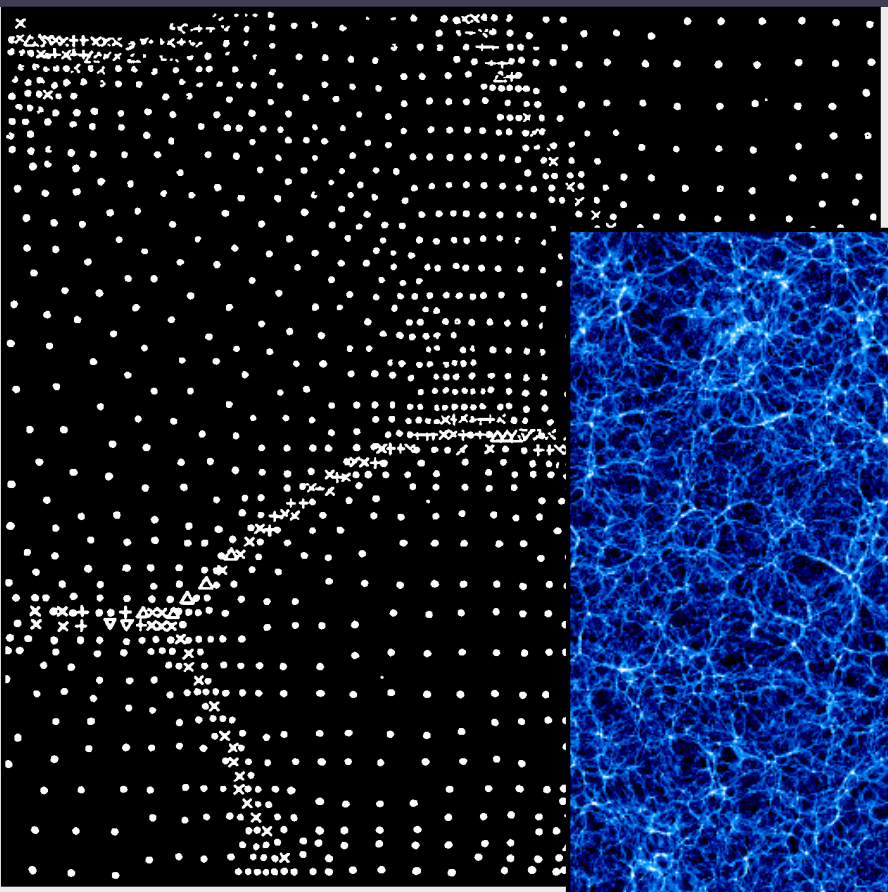


Sloan Foundation Telescope

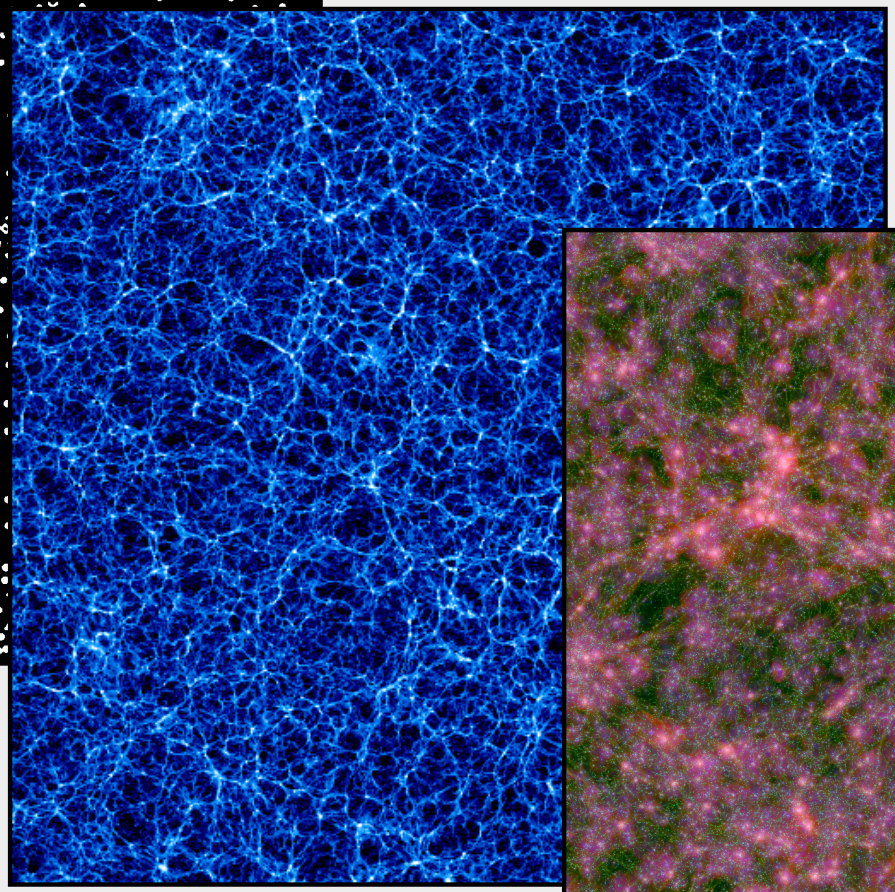
The Cosmic web

. . . to theory

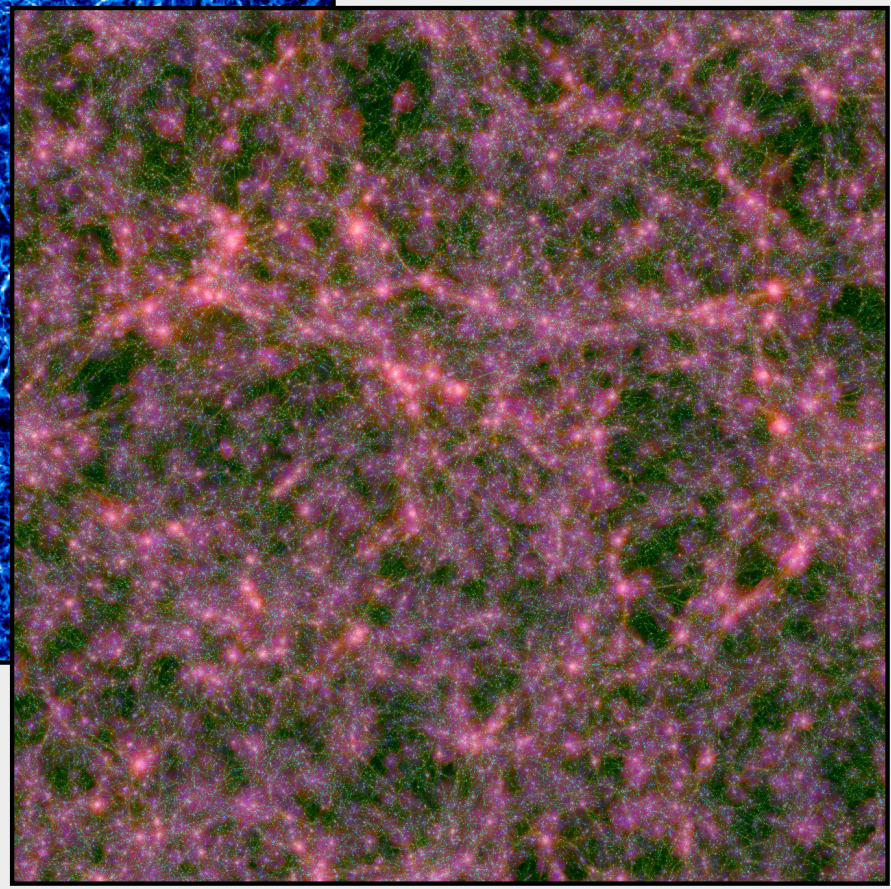
Klypin & Shandarin 1993
Bond, Kofman & Pogosyan 1996



Doroshkevich & Shandarin 1978
Zel'dovich 1970



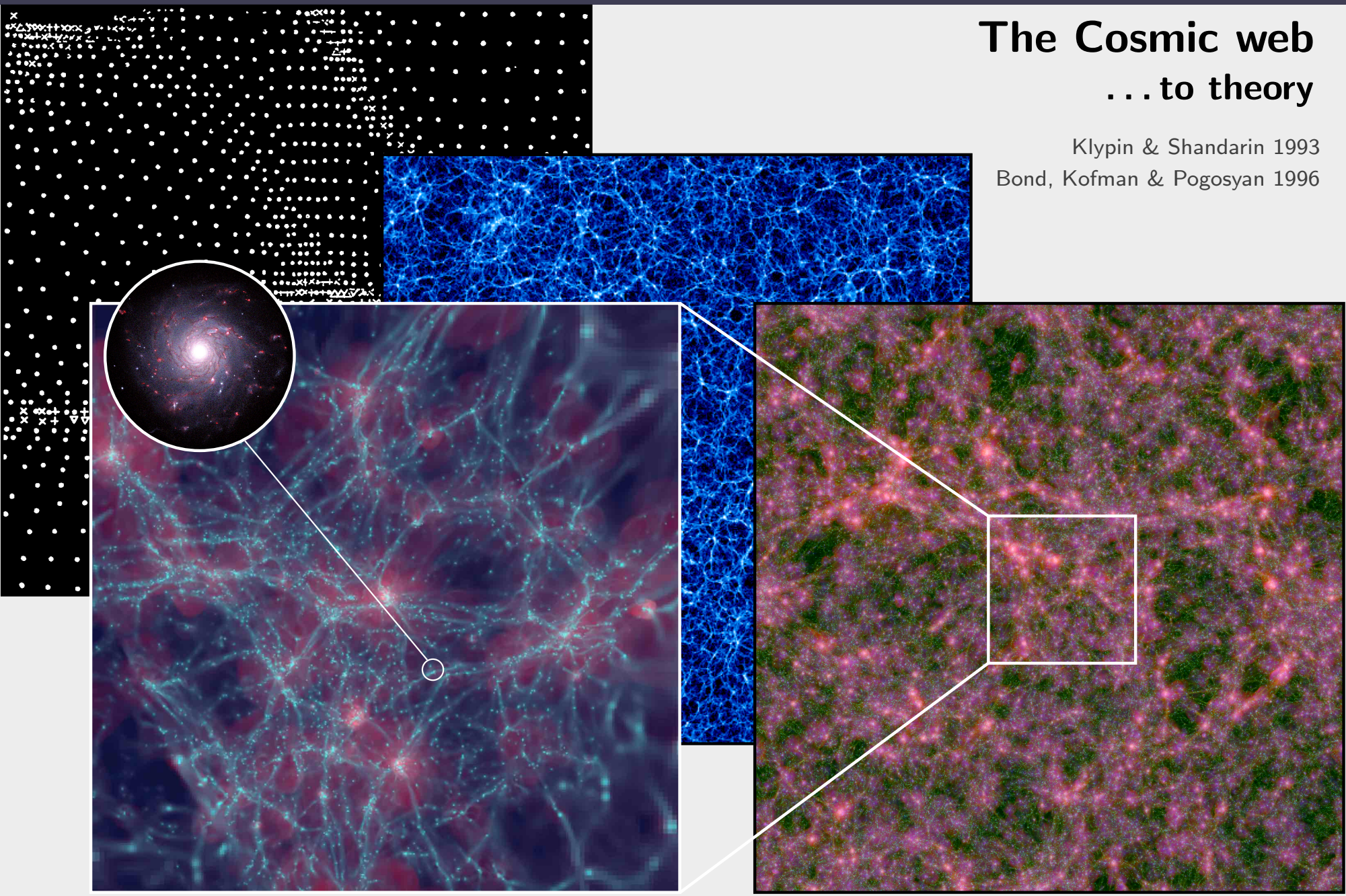
Marenostrum • Yepes et al. 2007



Horizon-AGN • Dubois et al. 2014

The Cosmic web
. . . to theory

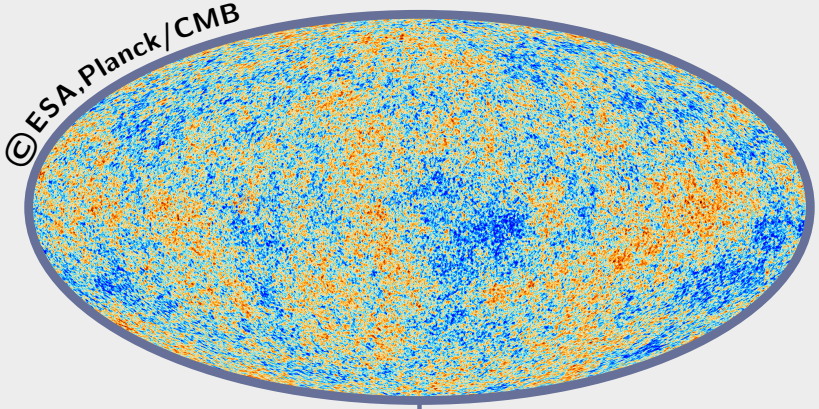
Klypin & Shandarin 1993
Bond, Kofman & Pogosyan 1996

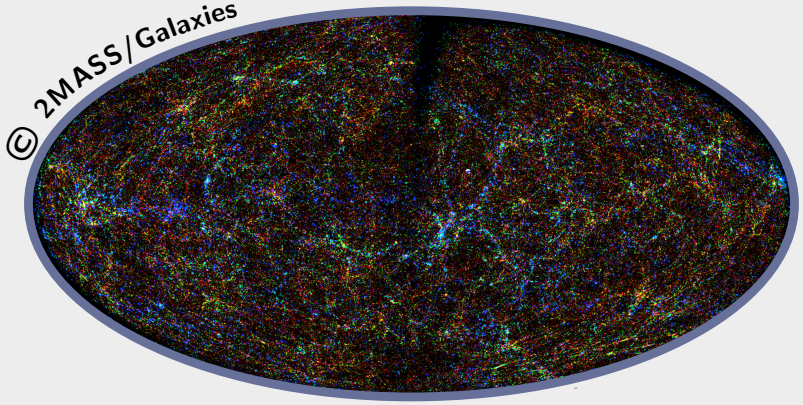


NewHorizon • Dubois et al. 2021

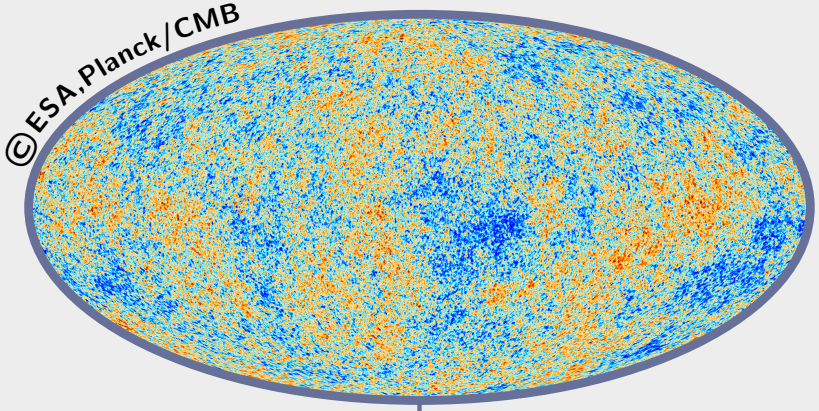
Horizon-AGN • Dubois et al. 2014

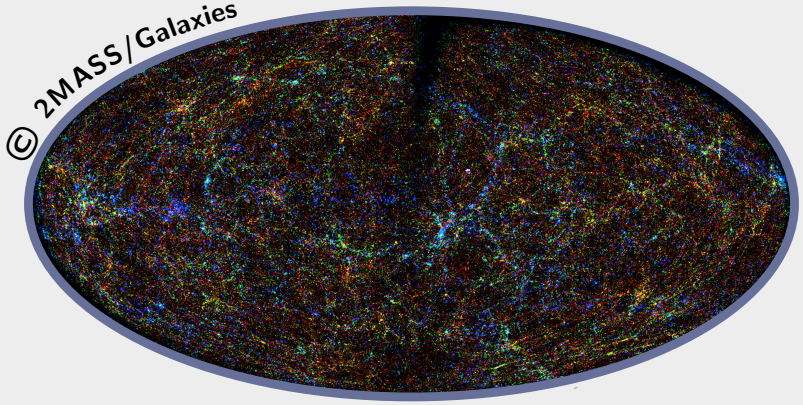
The Multi-scale Universe





The Multi-scale Universe

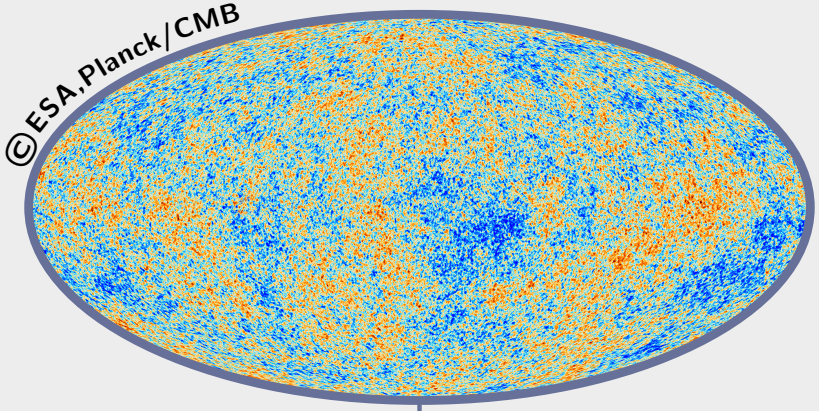


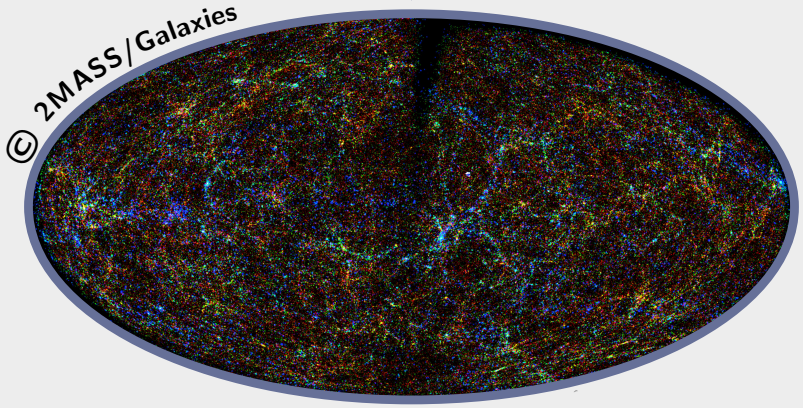


Theory

1. cosmological models
   - Gaussian random field (standard model) vs primordial non-Gaussianities
   - massive neutrinos
   - dark energy models ...
2. galaxy formation models
   - gravitational clustering
   - baryonic physics (scale-coupling) ...

The Multi-scale Universe





Theory

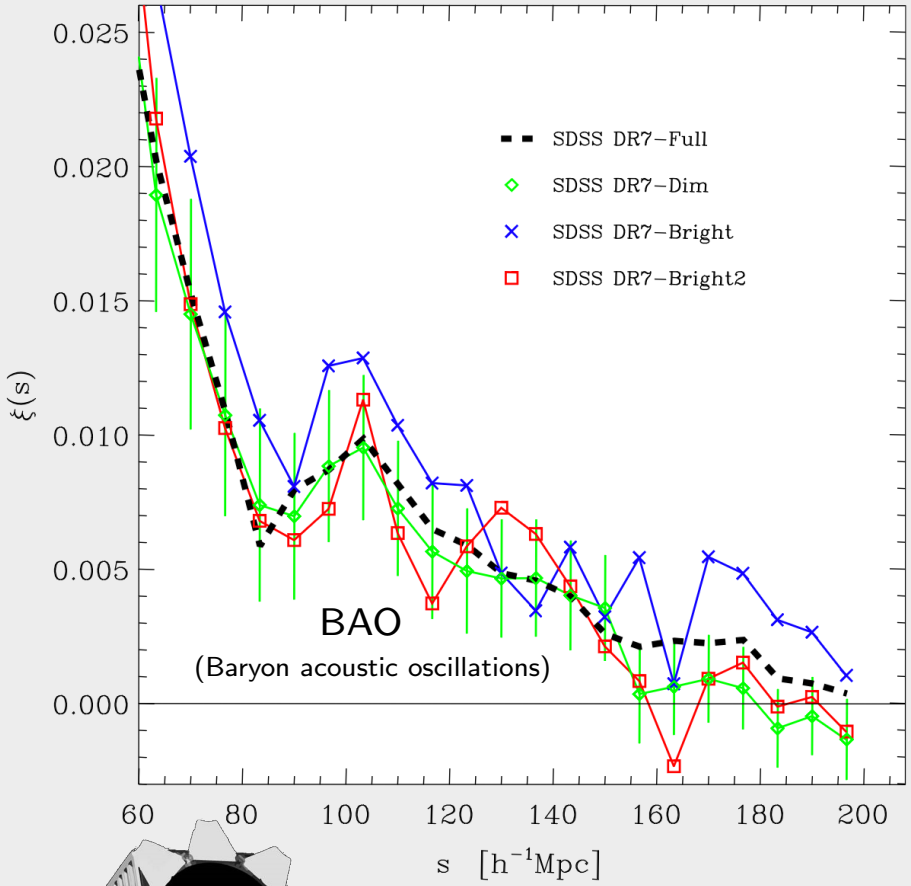
1. cosmological models
   - Gaussian random field (standard model) vs primordial non-Gaussianities
   - massive neutrinos
   - dark energy models ...
2. galaxy formation models
   - gravitational clustering
   - baryonic physics (scale-coupling) ...

Method

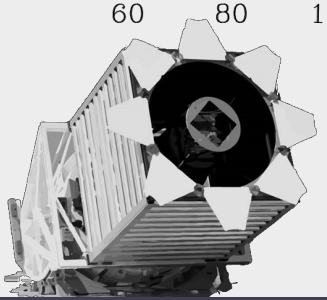
1. statistical measures
   - two-point correlation function
   - higher-order correlations
   - topological/geometrical descriptors ...
2. observables
   - galaxies
   - galaxy clusters
   - CMB ...

Characterisation of Large-scale structure

2-point correlation function



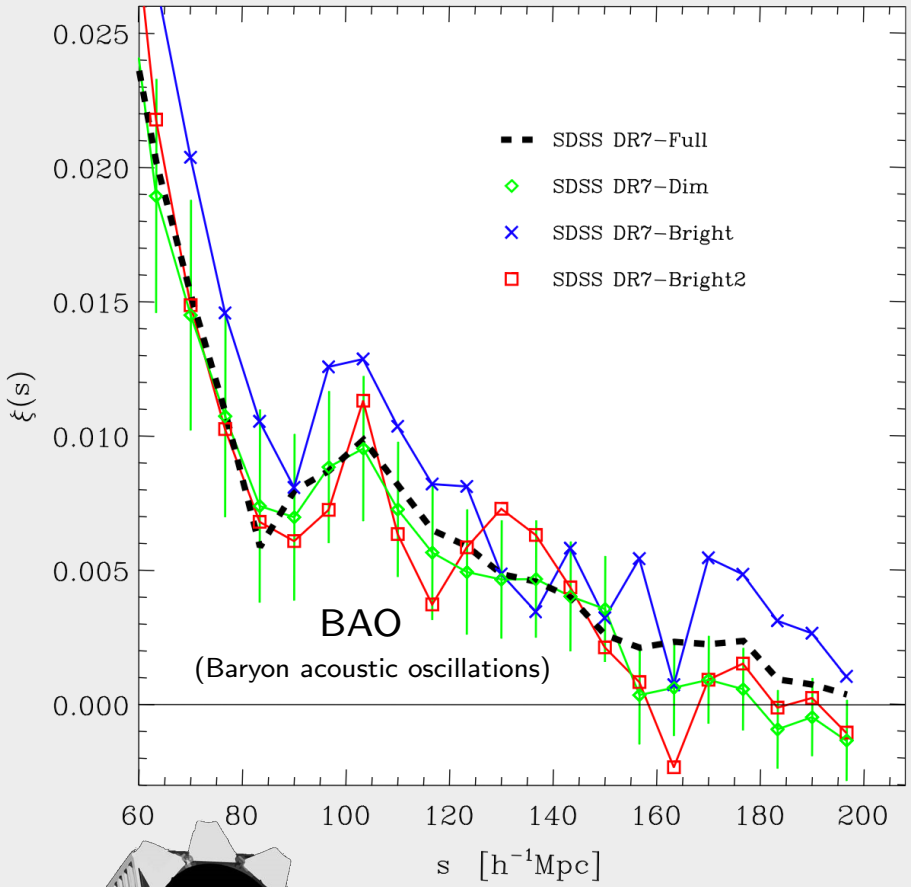
Kazin et al. 2010



SDSS

Characterisation of Large-scale structure

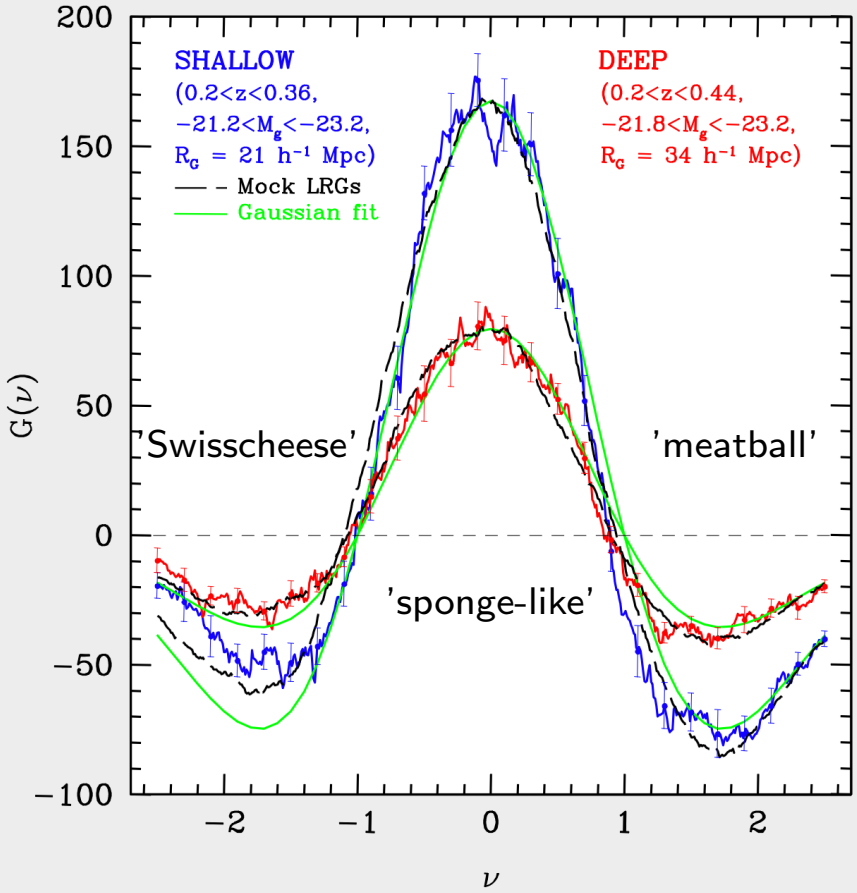
2-point correlation function



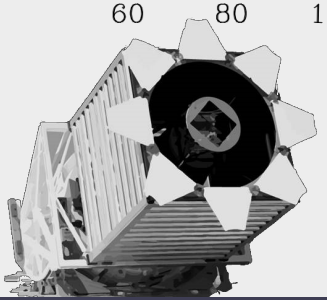
Kazin et al. 2010

Genus topology

(# of holes - # of isolated regions)



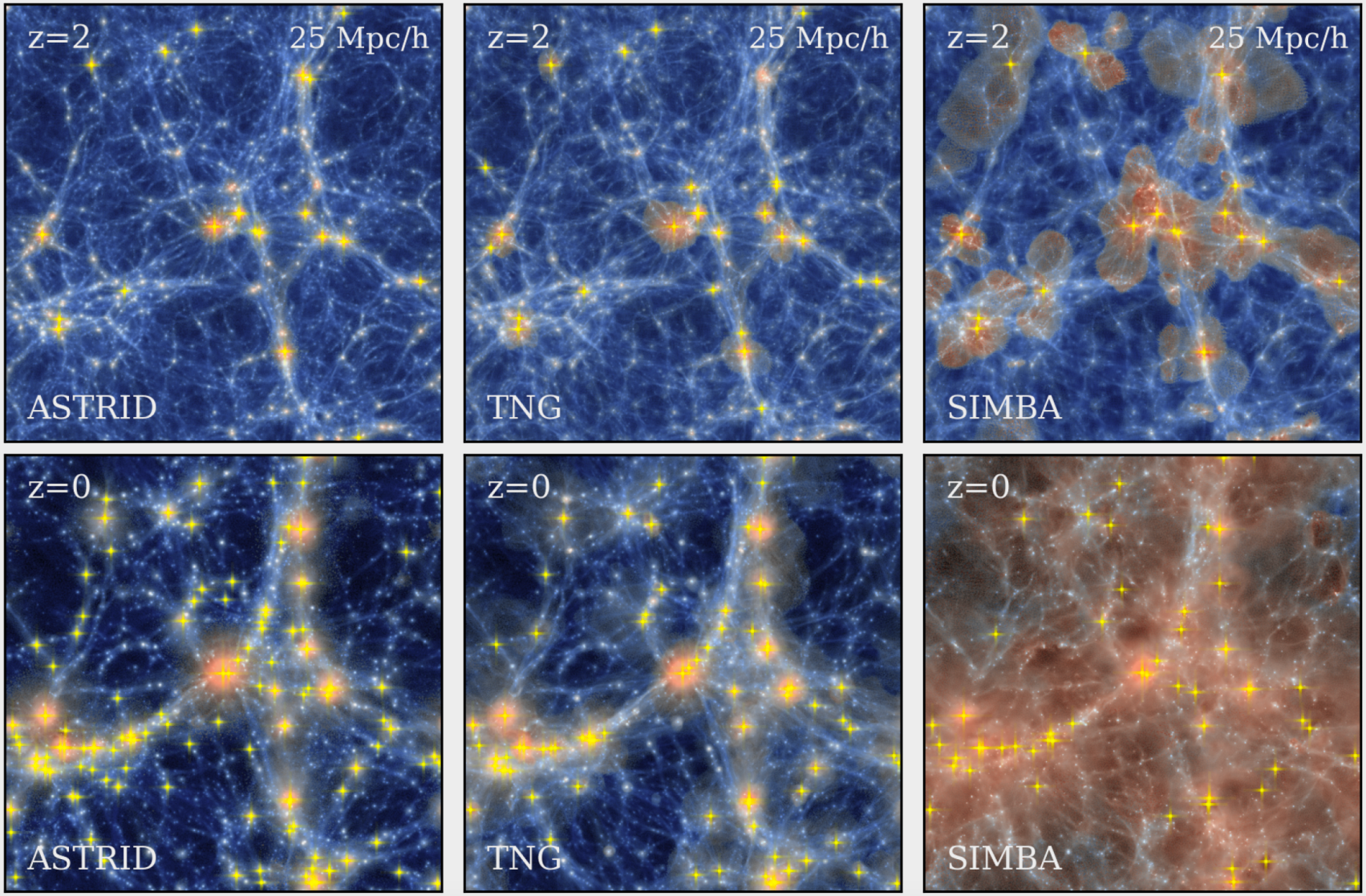
Gott et al. 2009



SDSS

Baryonic processes

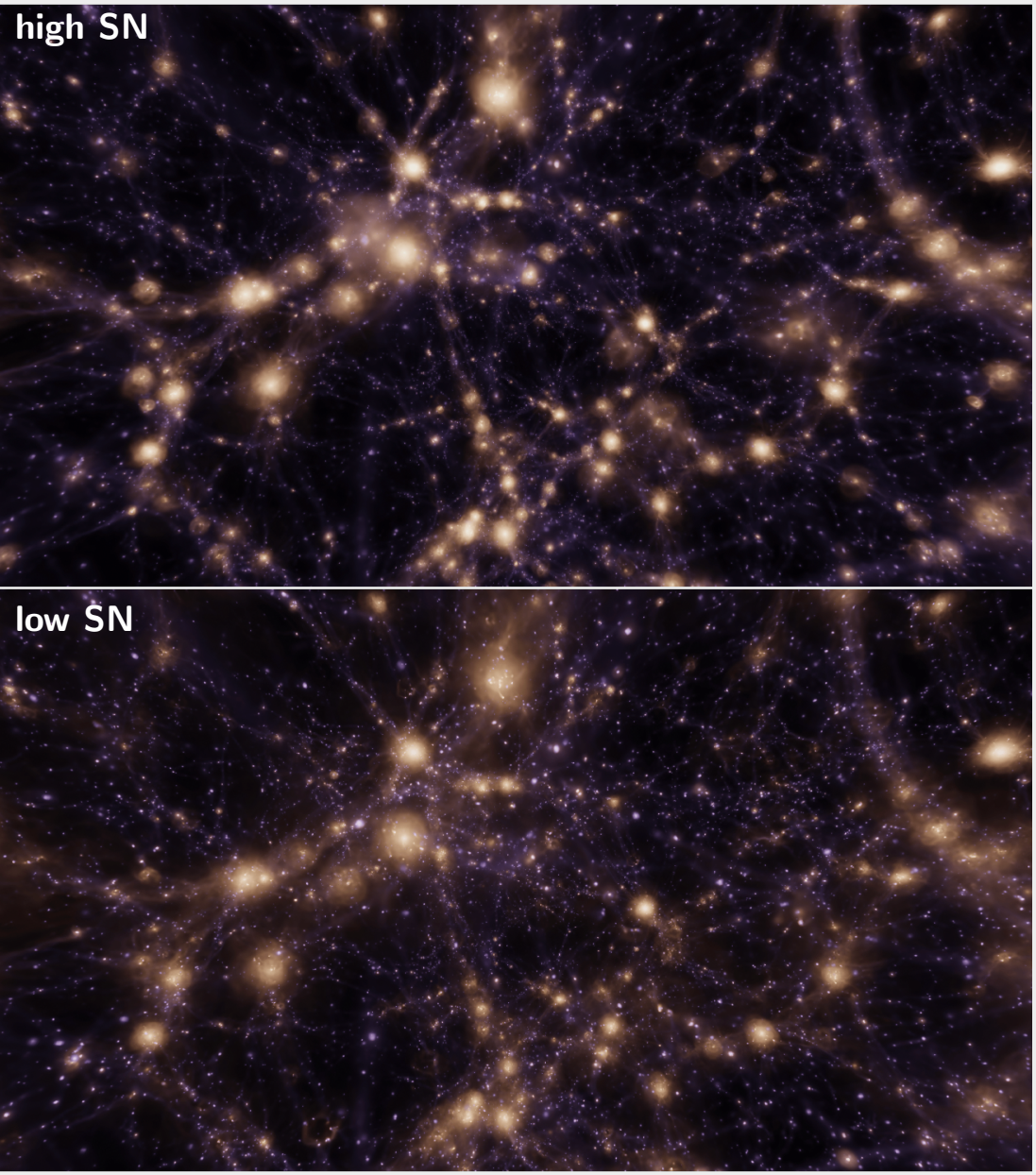
Gas temperature



CAMELS • Ni et al. 2023

Baryonic processes
Gas density & temperature

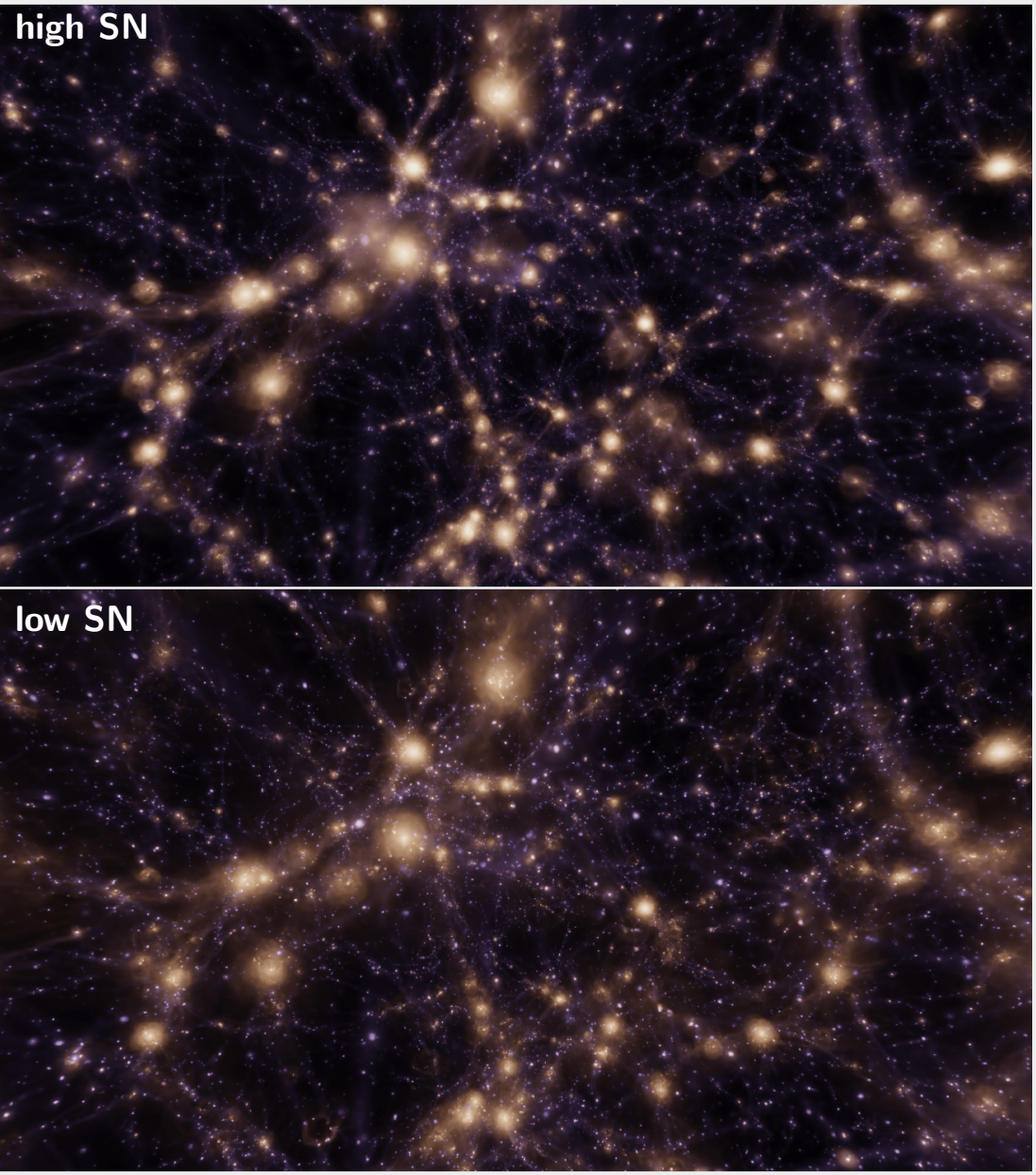
IllustrisTNG



CAMELS • Villaescusa-Navarro et al. 2022

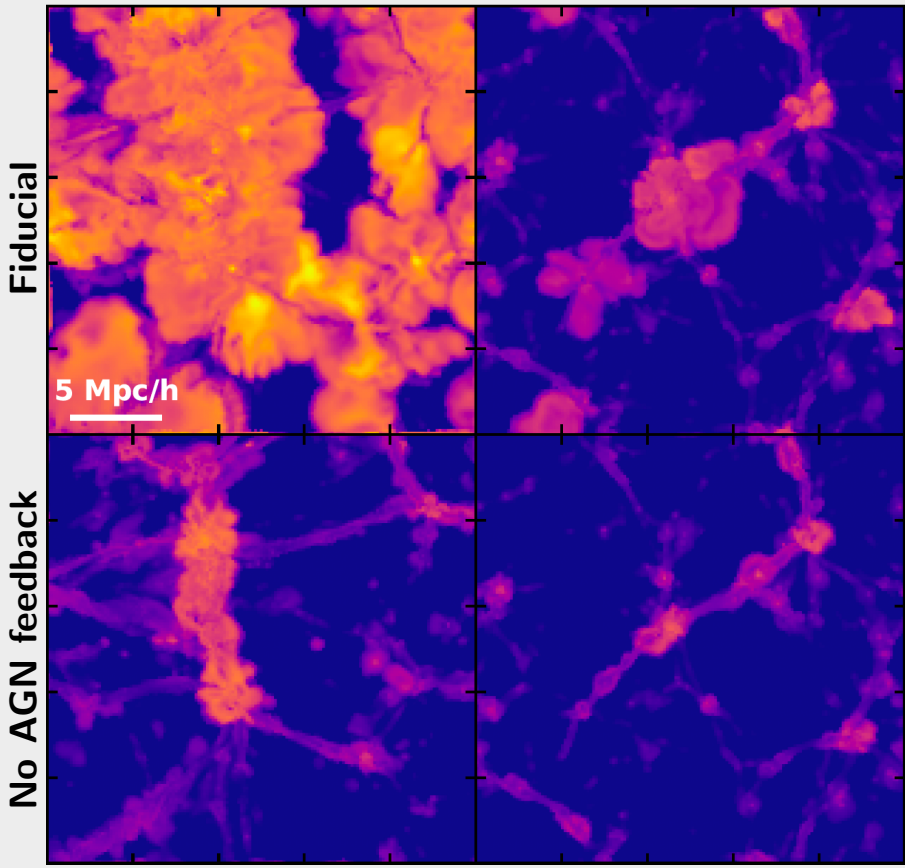
Baryonic processes
Gas density & temperature

IllustrisTNG



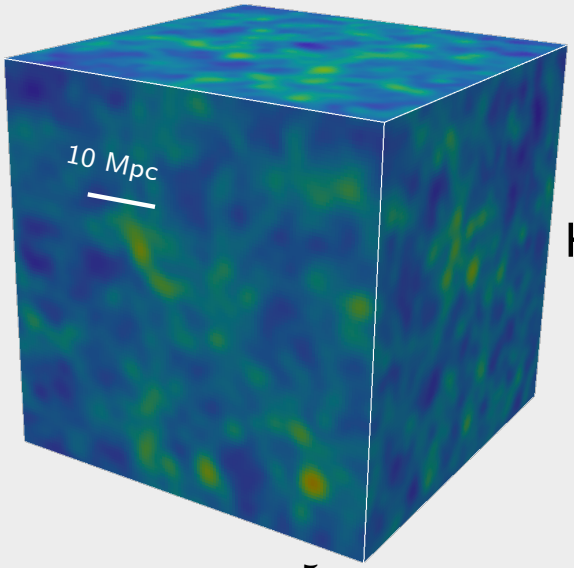
CAMELS • Villaescusa-Navarro et al. 2022

Simba IllustrisTNG



Tillmann et al. 2023

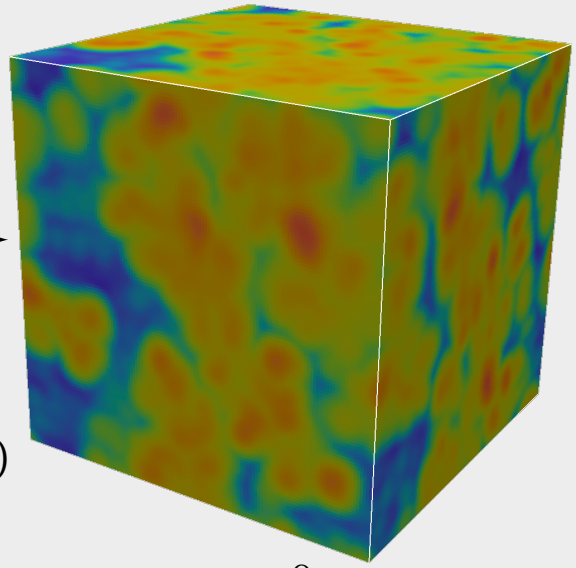
Baryonic physics on large scales



z $= 5$

cosmic evolution

cooling, heating
chemistry (11 elements)
dust growth & destruction
HI & H_2 fractions (on the fly)
star formation (H_2-based)
black holes

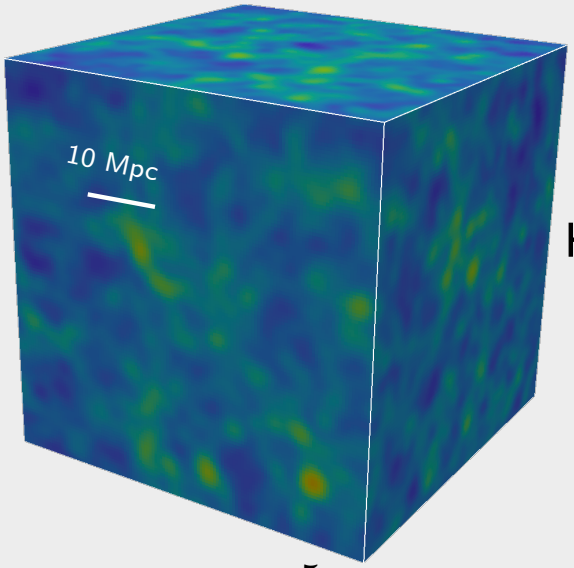


z $= 0$

Temperature

SIMBA • Davé et al. 2019

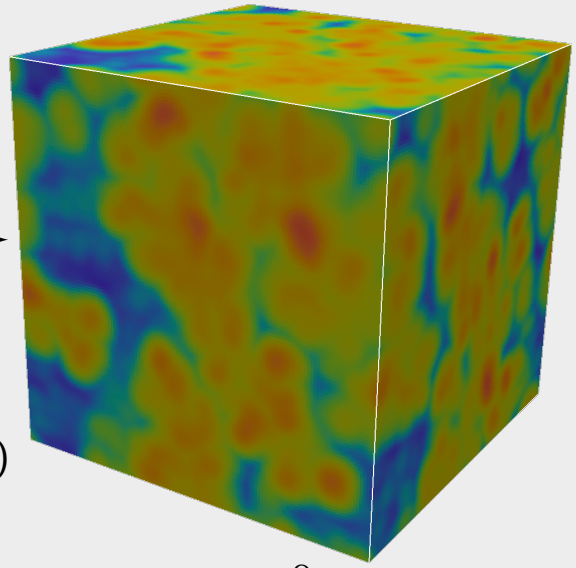
Baryonic physics on large scales



z = 5

cosmic evolution

cooling, heating
chemistry (11 elements)
dust growth & destruction
HI & H_2 fractions (on the fly)
star formation (H_2-based)
black holes



z = 0

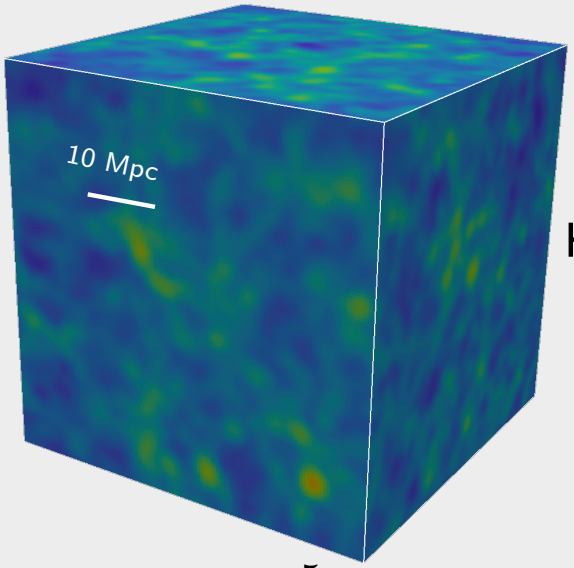
Temperature

	Fiducial
Stellar feedback	✓
AGN winds	✓
Jets	✓
X-ray heating	✓

Summary of main ingredients of different SIMBA runs

SIMBA • Davé et al. 2019

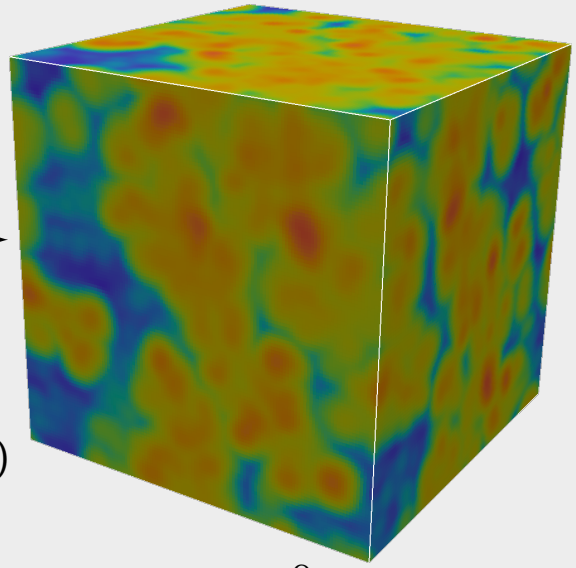
Baryonic physics on large scales



z = 5

cosmic evolution

cooling, heating
chemistry (11 elements)
dust growth & destruction
HI & H_2 fractions (on the fly)
star formation (H_2-based)
black holes



z = 0

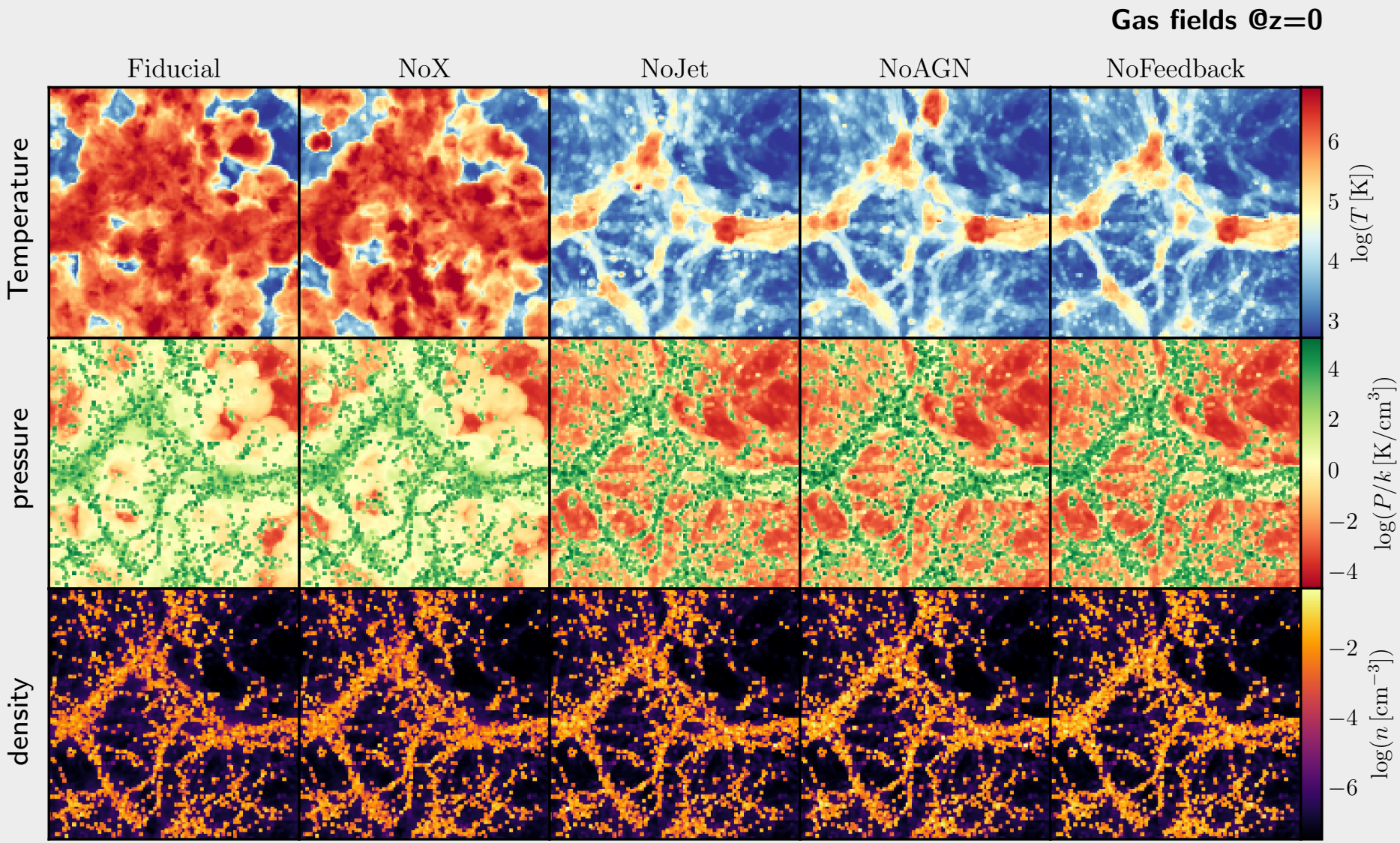
Temperature

	Fiducial	NoX	NoJet	NoAGN	NoFeedback
Stellar feedback	✓	✓	✓	✓	
AGN winds	✓	✓	✓		
Jets	✓	✓			
X-ray heating	✓				

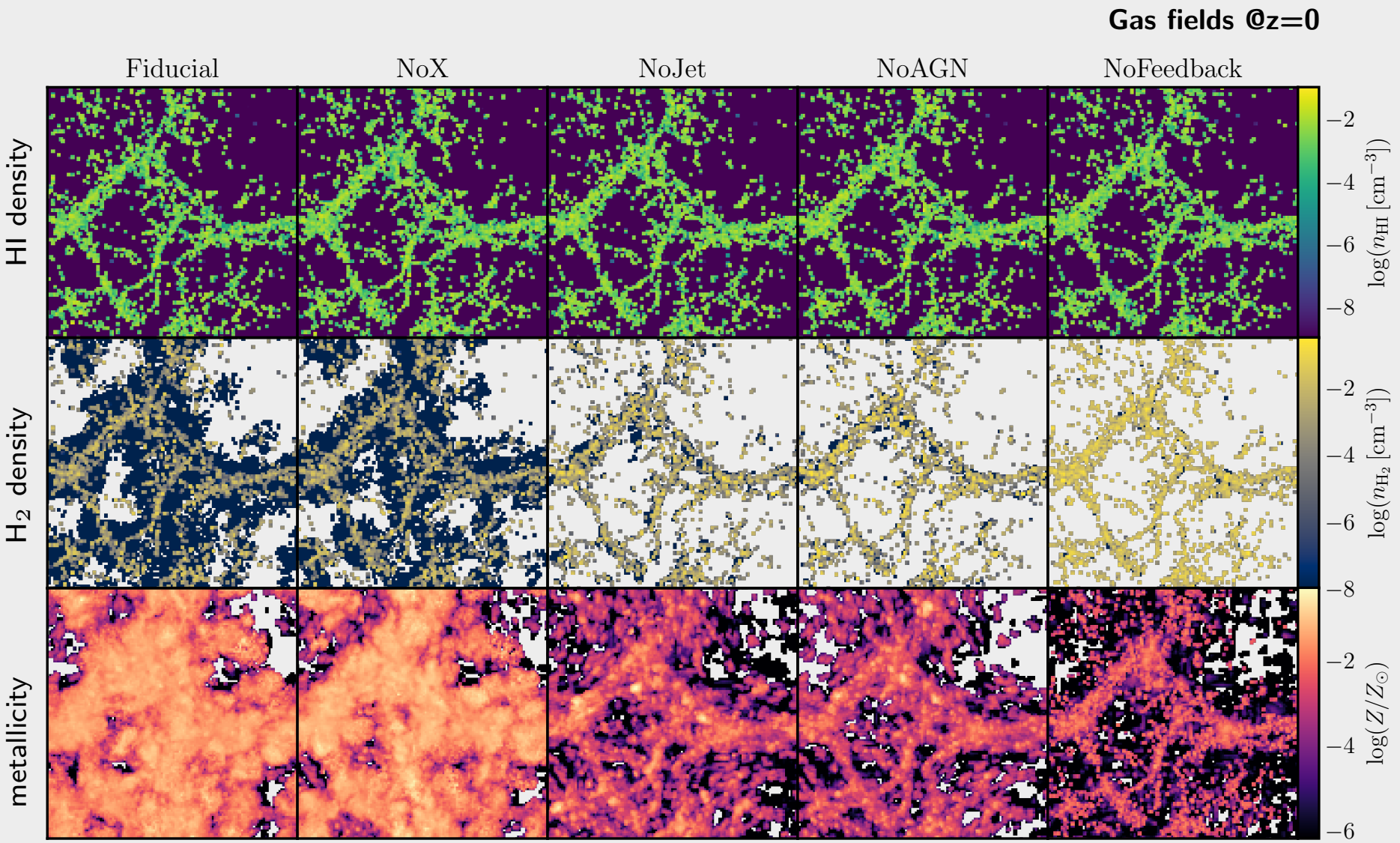
Summary of main ingredients of different SIMBA runs

SIMBA • Davé et al. 2019

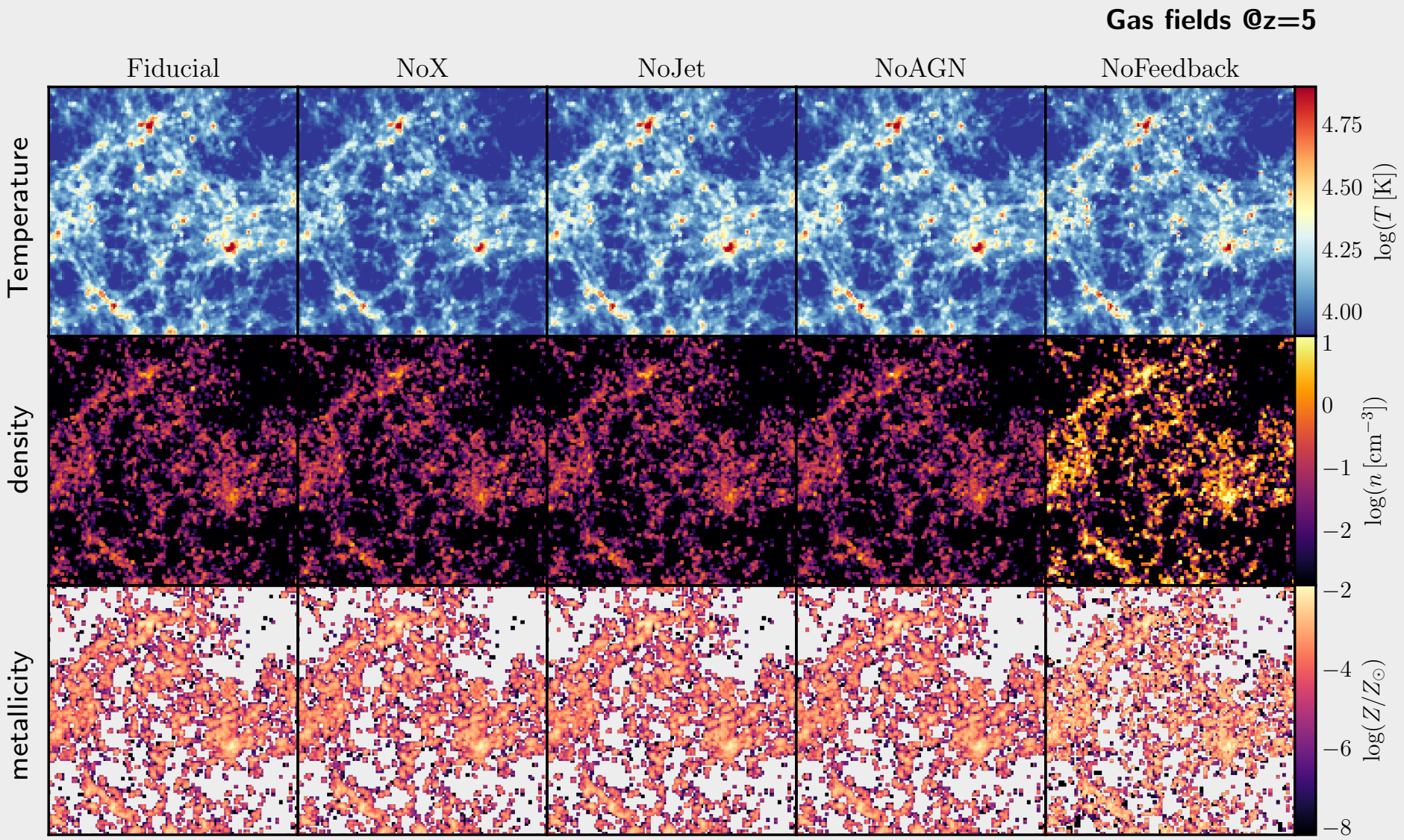
Baryonic physics on large scales



Baryonic physics on large scales



Baryonic physics on large scales



Morphology on large scales

- random field $f(\mathbf{x})$ on a d-dimensional support $\mathcal{D} \subseteq \mathbb{R}^d$

  $\rightarrow C_\theta$ - excursion set for a given threshold θ

$$C_\theta = \{\mathbf{x} \in \mathcal{D} | f(\mathbf{x}) \geq \theta\}$$

Morphology on large scales

- random field $f(\mathbf{x})$ on a d-dimensional support $\mathcal{D} \subseteq \mathbb{R}^d$

  $\rightarrow C_\theta$ - excursion set for a given threshold θ

  $$C_\theta = \{\mathbf{x} \in \mathcal{D} | f(\mathbf{x}) \geq \theta\}$$

  $\rightarrow$ Minkowski functionals (per unit volume) for $d = 3$:

  $$v_0(\theta) = \frac{1}{\mathcal{V}} \int_{C_\theta} dV(\mathbf{x}) \quad \ldots \text{ volume}$$

  $$v_1(\theta) = \frac{1}{6}\frac{1}{\mathcal{V}} \int_{\partial C_\theta} dA(\mathbf{x}) \quad \ldots \text{ surface area}$$

  $$v_2(\theta) = \frac{1}{6\pi}\frac{1}{\mathcal{V}} \int_{\partial C_\theta} dA(\mathbf{x}) \left(\frac{1}{R_1(\mathbf{x})} + \frac{1}{R_2(\mathbf{x})}\right) \quad \ldots \text{ mean curvature}$$

  $$v_3(\theta) = \frac{1}{4\pi}\frac{1}{\mathcal{V}} \int_{\partial C_\theta} dA(\mathbf{x}) \frac{1}{R_1(\mathbf{x}) R_2(\mathbf{x})} \quad \ldots \text{ Gaussian curvature}$$

where $dV(\mathbf{x})$, $dA(\mathbf{x})$ - elementary volume and area of the excursion sets of field f

with ∂C_θ - boundary surface

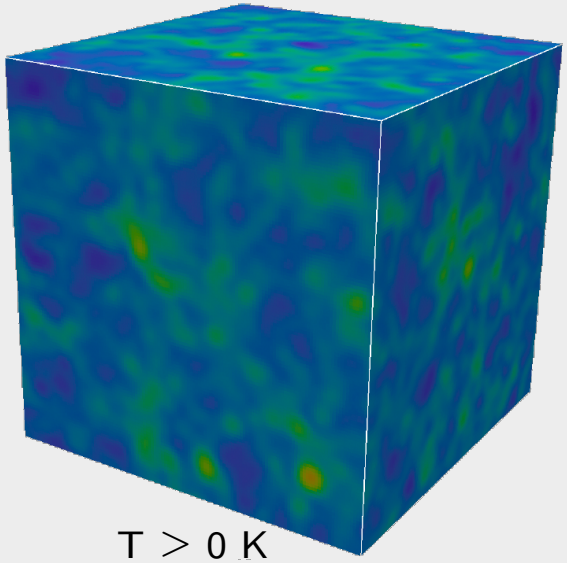
$R_{1,2}(\mathbf{x})$ - principal local curvature radii

Koenderink 1984

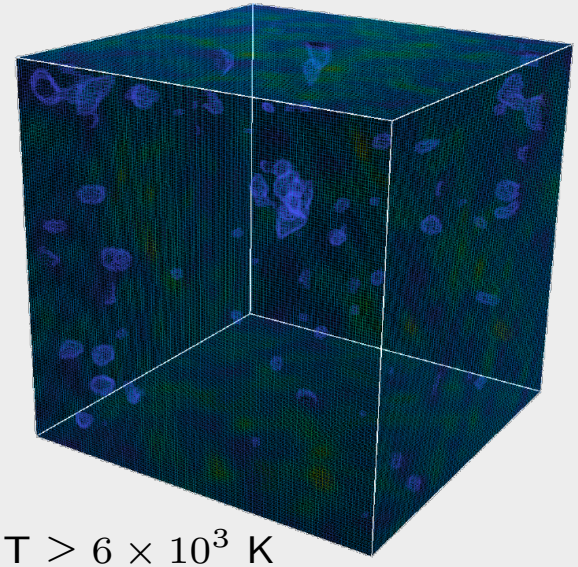
Schmalzing & Buchert 1997

Excursion sets

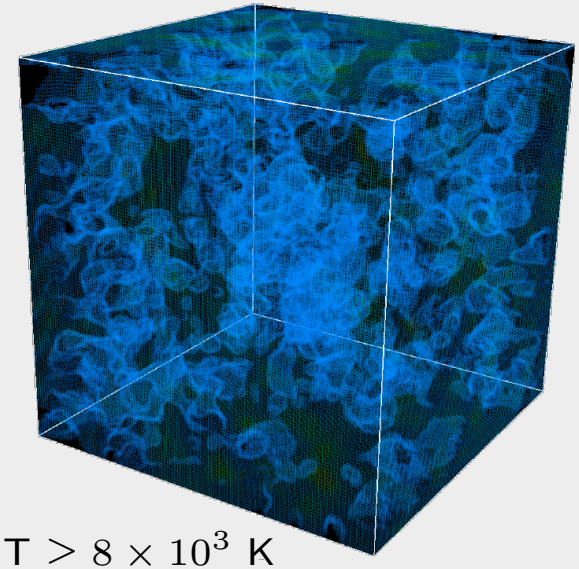
Gas temperature @z=5



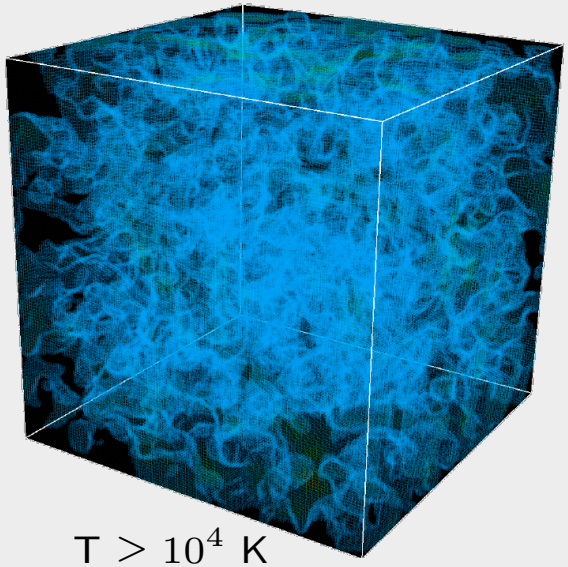
$T \geq 0$ K



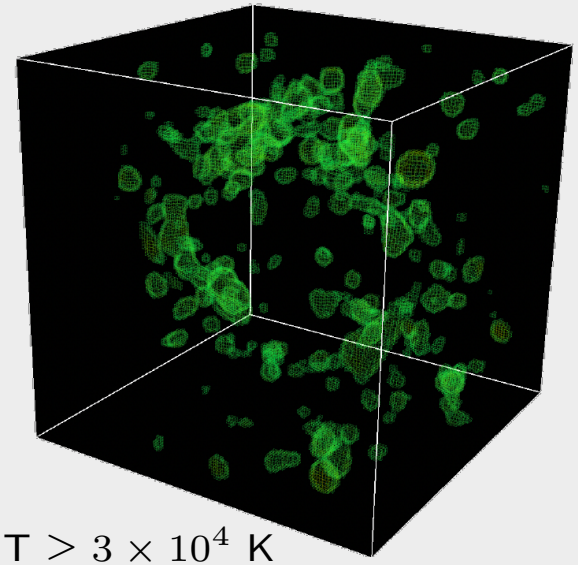
$T \geq 6 \times 10^3$ K



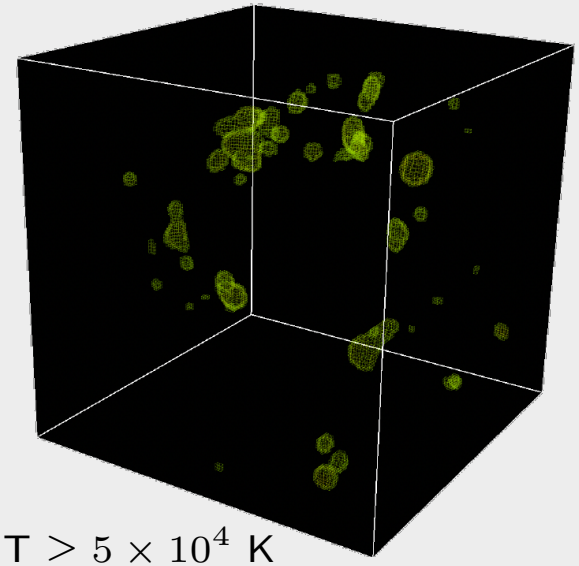
$T \geq 8 \times 10^3$ K



$T \geq 10^4$ K

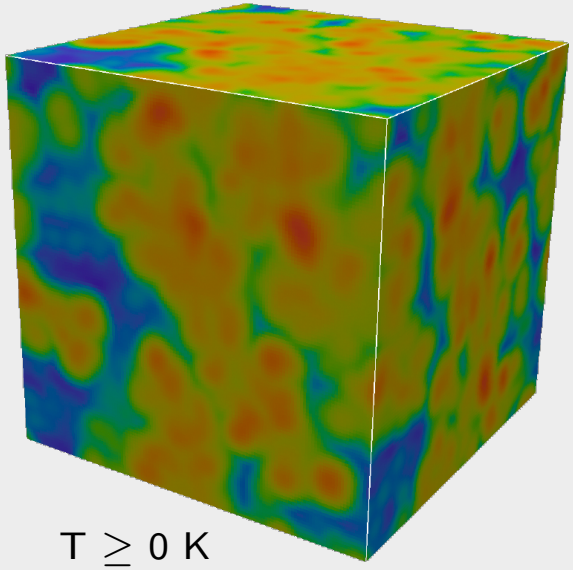


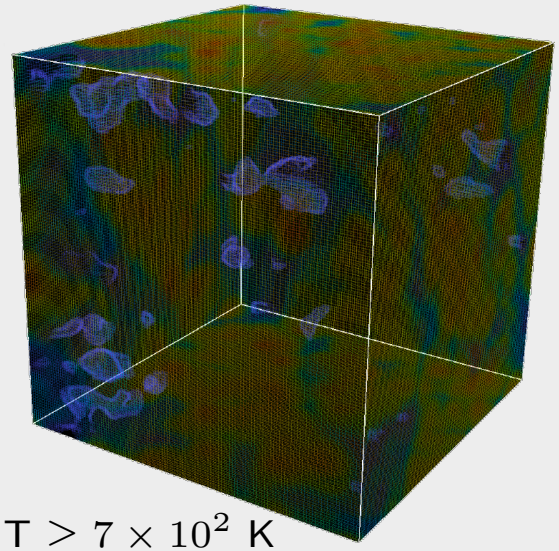
$T \geq 3 \times 10^4$ K

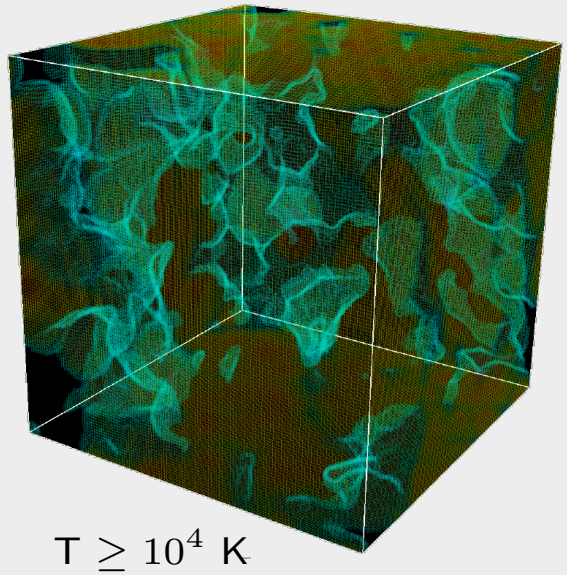


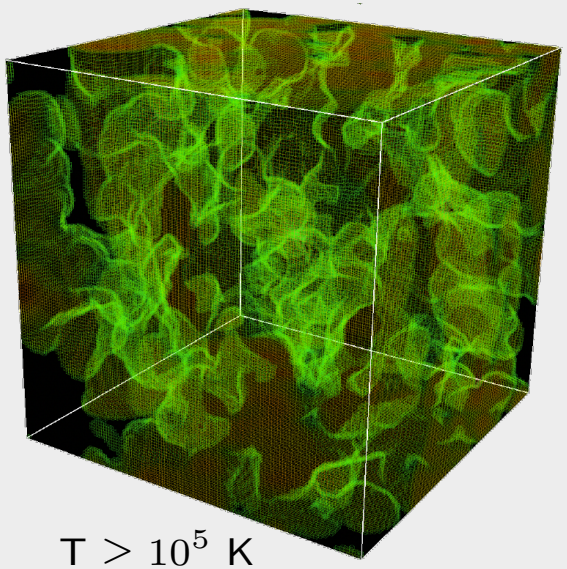
$T \geq 5 \times 10^4$ K

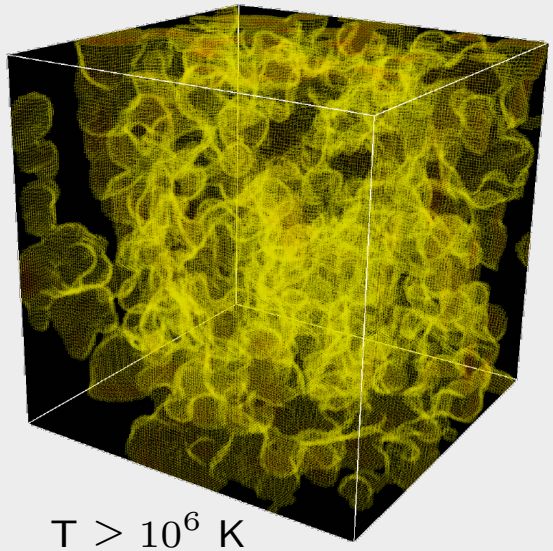
Gas temperature @z=0

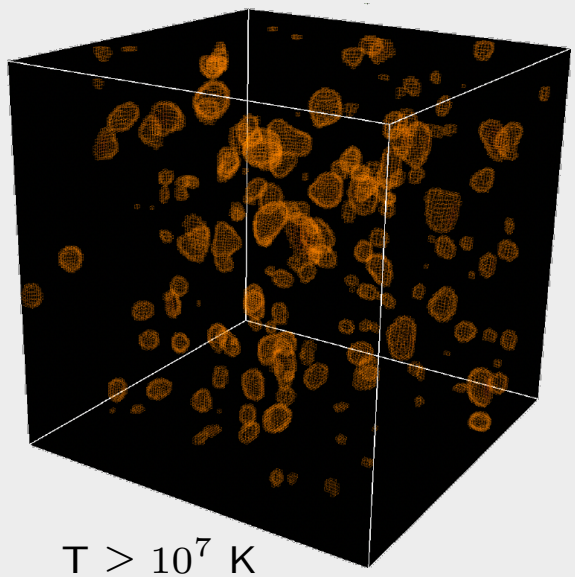




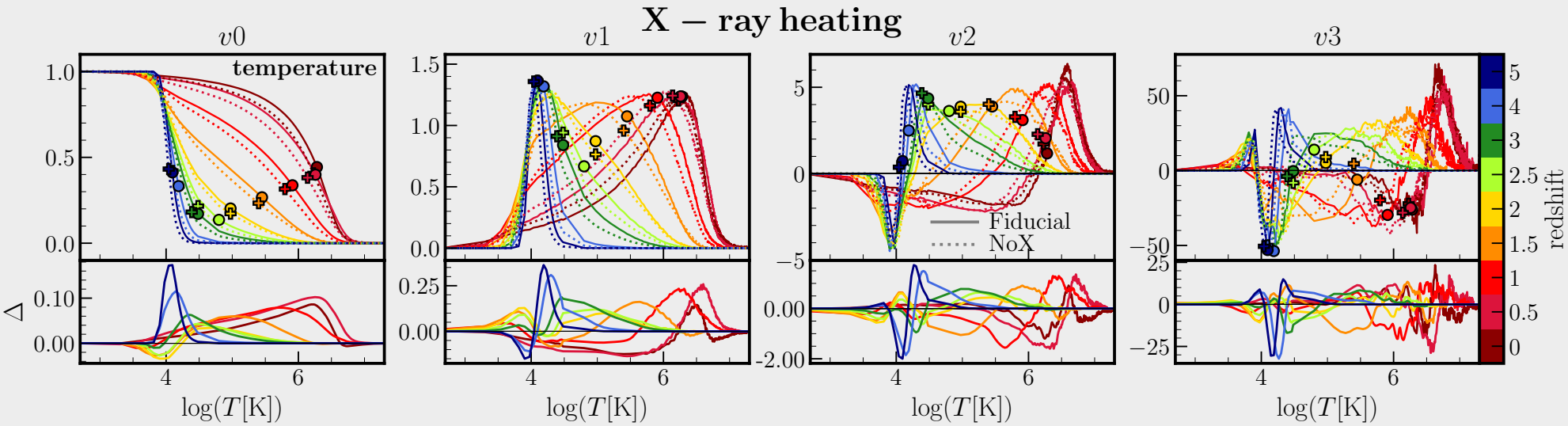




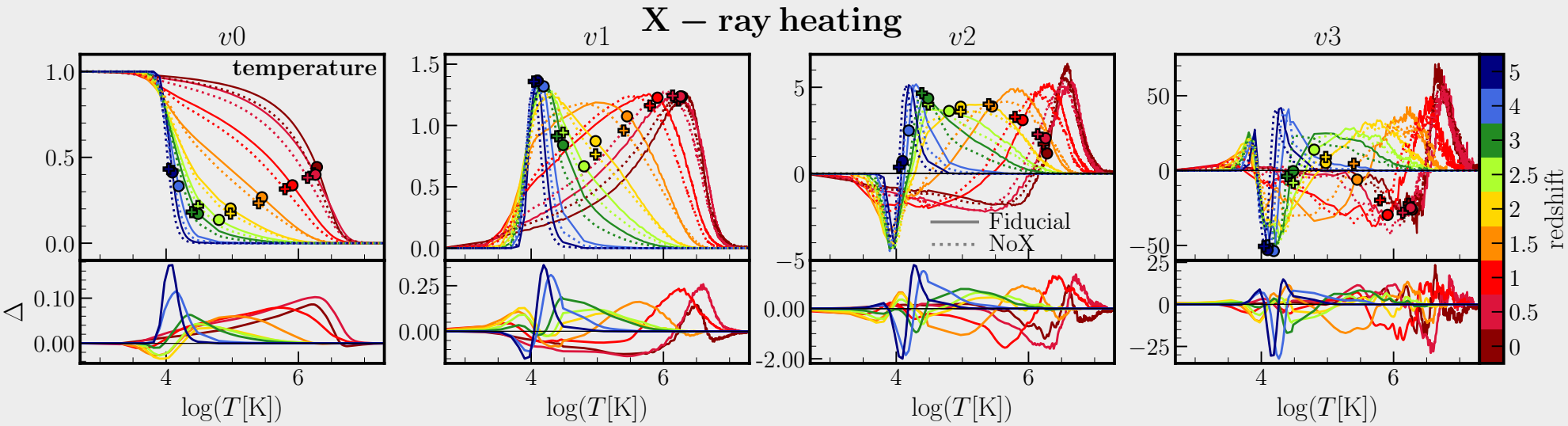




Temperature field



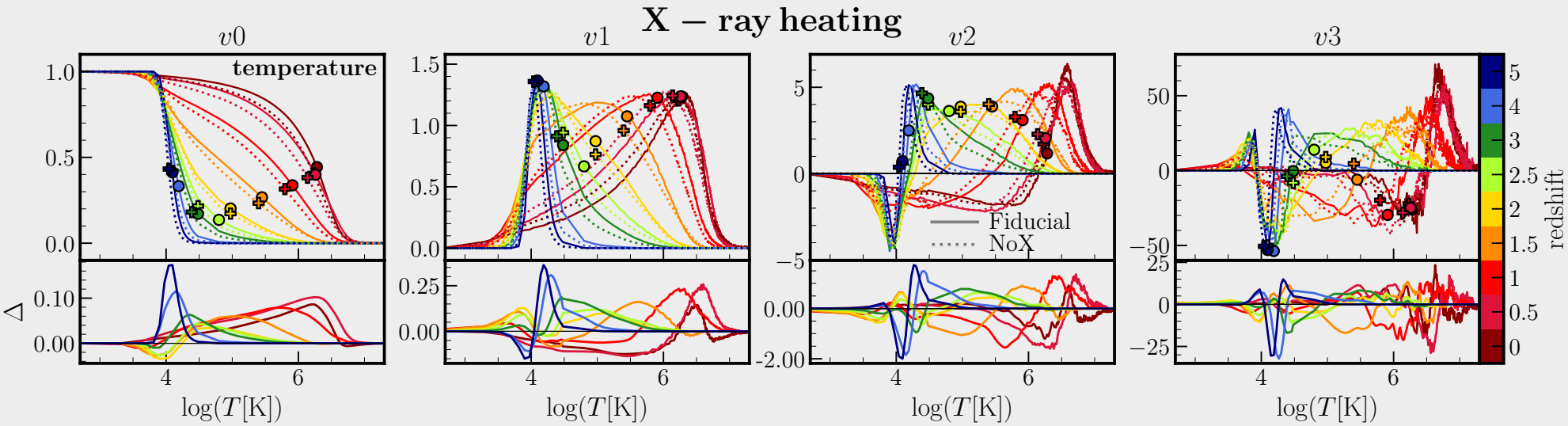
Temperature field



All feedbacks

- v0 : step-like function at $z > 4$ (single phase at T$\sim 10^4$K) & small fraction in hot regions

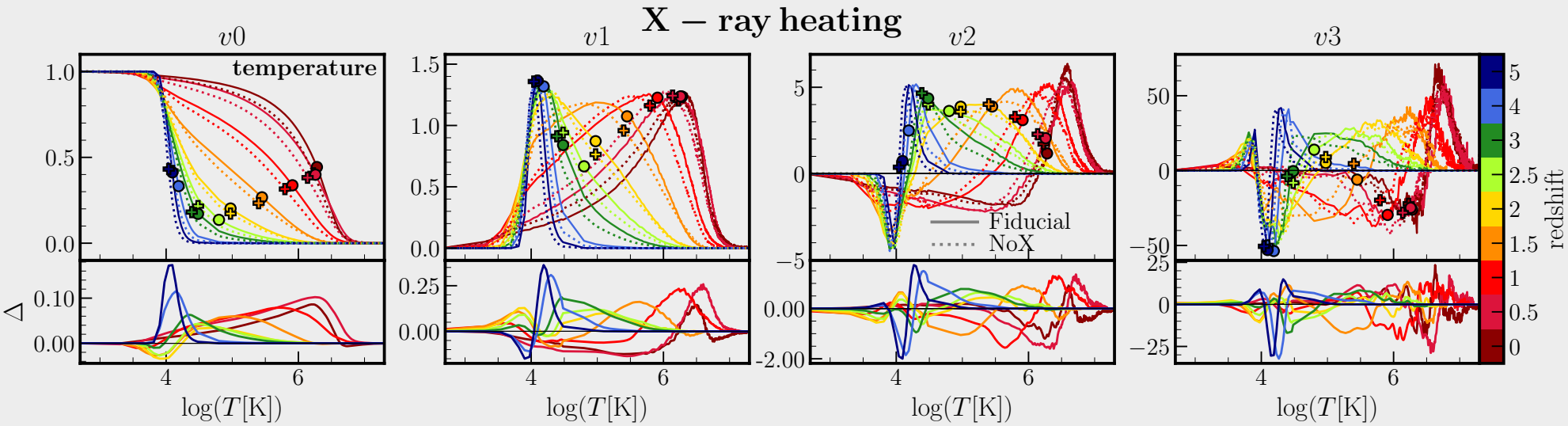
Temperature field



All feedbacks

- v0 : step-like function at $z > 4$ (single phase at T$\sim 10^4$K) & small fraction in hot regions
  : low z IGM strongly heated by AGN, stellar feedback and shock heating

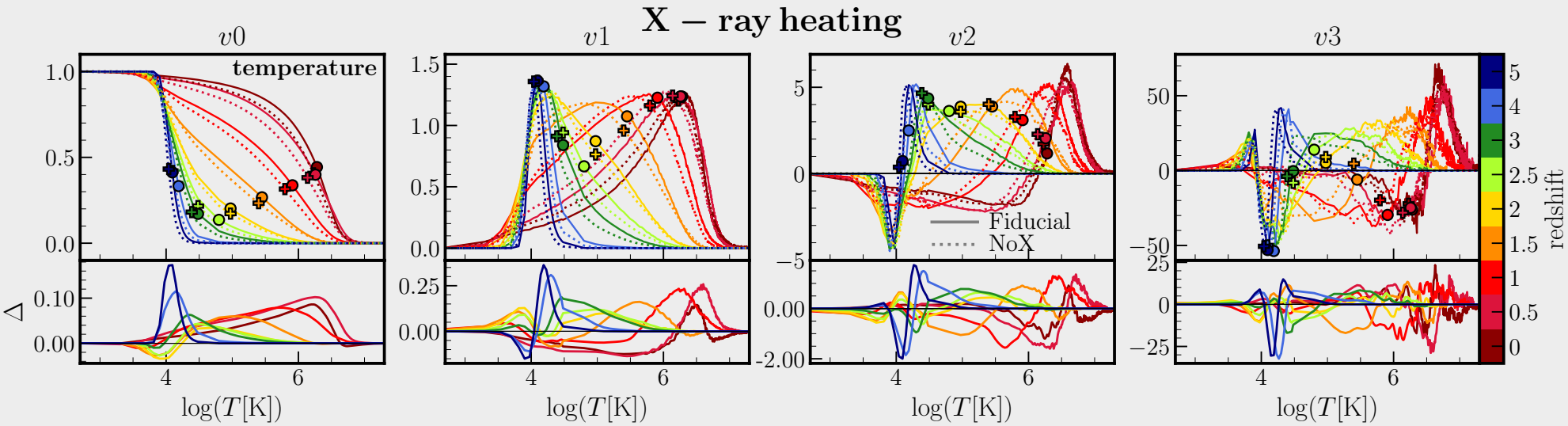
Temperature field



All feedbacks

- v0 : step-like function at $z > 4$ (single phase at T$\sim 10^4$K) & small fraction in hot regions
  : low z IGM strongly heated by AGN, stellar feedback and shock heating
- v1 : symmetric and peaked at T$\sim 10^4$K at high z; right-tailed until $z \sim 2$

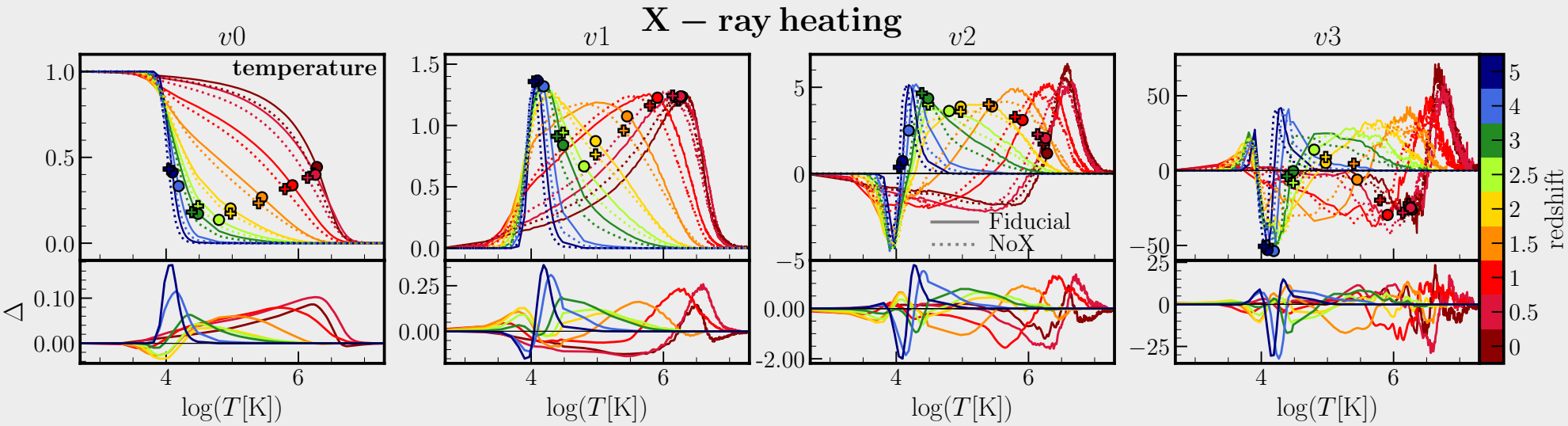
Temperature field



All feedbacks

- v0 : step-like function at $z > 4$ (single phase at T$\sim 10^4$K) & small fraction in hot regions
  : low z IGM strongly heated by AGN, stellar feedback and shock heating
- v1 : symmetric and peaked at T$\sim 10^4$K at high z; right-tailed until $z \sim 2$
  : left-tailed at $z < 2$, dominated by T$<\bar{\mathrm{T}}$ ($\bar{\mathrm{T}} \sim 10^6$K at $z = 0$)

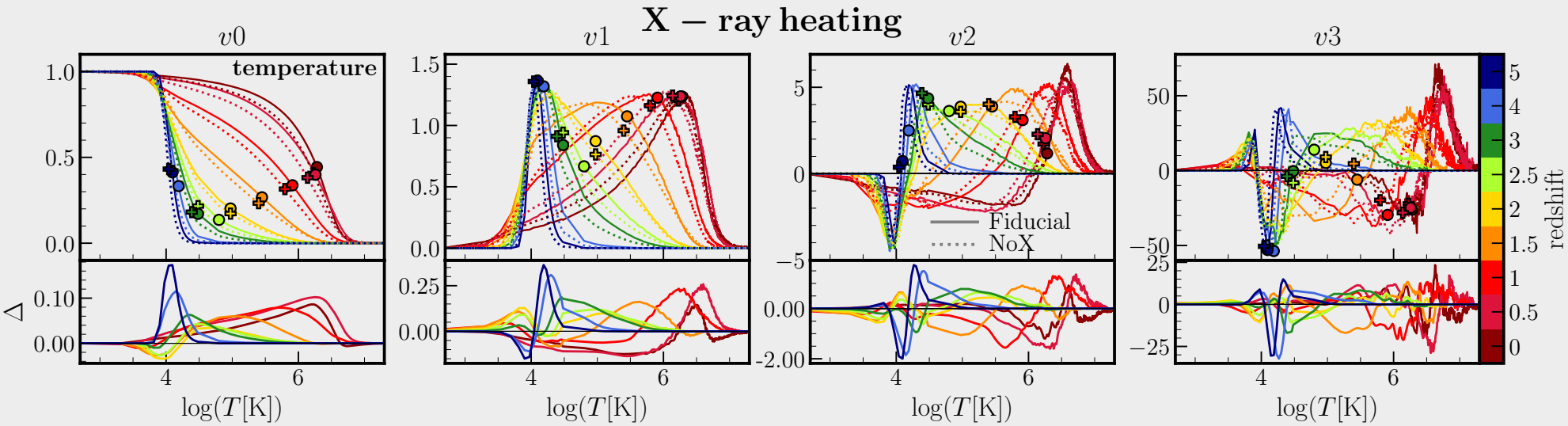
Temperature field



All feedbacks

- v0 : step-like function at $z > 4$ (single phase at T$\sim 10^4$K) & small fraction in hot regions
  : low z IGM strongly heated by AGN, stellar feedback and shock heating
- v1 : symmetric and peaked at T$\sim 10^4$K at high z; right-tailed until $z \sim 2$
  : left-tailed at $z < 2$, dominated by T$<\bar{\text{T}}$ ($\bar{\text{T}} \sim 10^6$K at $z = 0$)
- v2 & v3 : concave (v2 < 0) & dominated by tunnels (v3 < 0) at $z = 1$ for $T \gtrsim 10^4$K; $z = 0.5$ for $T \gtrsim 10^5$K (network of cold filaments in a warm percolating IGM)

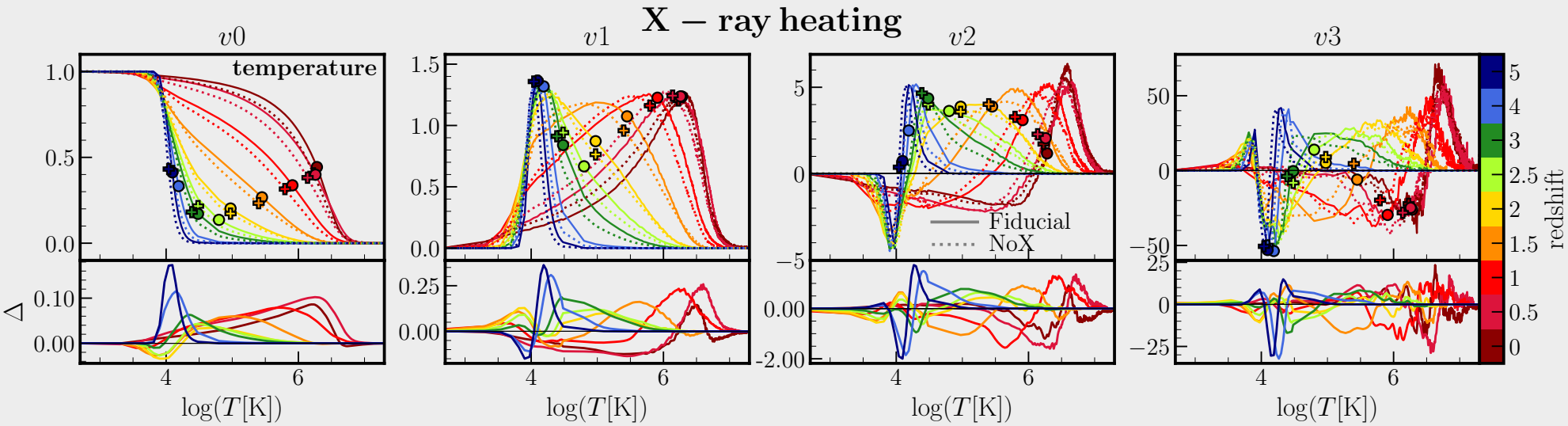
Temperature field



All feedbacks

- v0 : step-like function at $z > 4$ (single phase at T$\sim 10^4$K) & small fraction in hot regions
  : low z IGM strongly heated by AGN, stellar feedback and shock heating
- v1 : symmetric and peaked at T$\sim 10^4$K at high z; right-tailed until $z \sim 2$
  : left-tailed at $z < 2$, dominated by T$<\bar{\text{T}}$ ($\bar{\text{T}} \sim 10^6$K at $z = 0$)
- v2 & v3 : concave (v2 < 0) & dominated by tunnels (v3 < 0) at $z = 1$ for $T \gtrsim 10^4$K; $z = 0.5$ for $T \gtrsim 10^5$K (network of cold filaments in a warm percolating IGM)
  : $z = 0$, concave regions with T$< 10^{5.5}$K with vanishing v3 (cold bubbles)

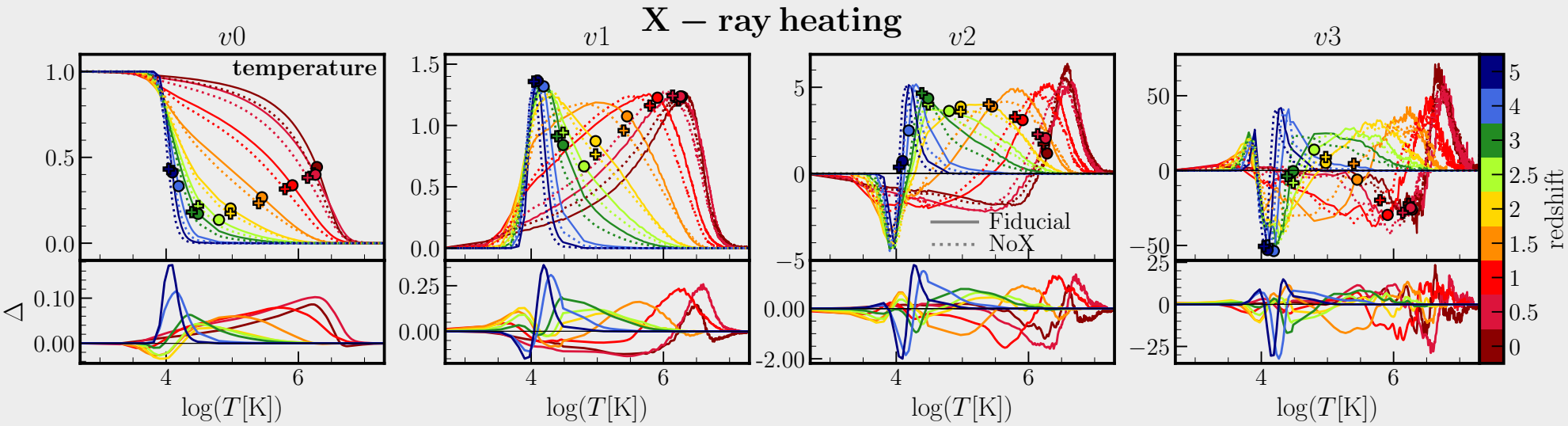
Temperature field



X-ray heating

- 2 epochs: $z > 4$ on cold (T $\simeq 10^4$K) gas (heating or removal of cold gas)

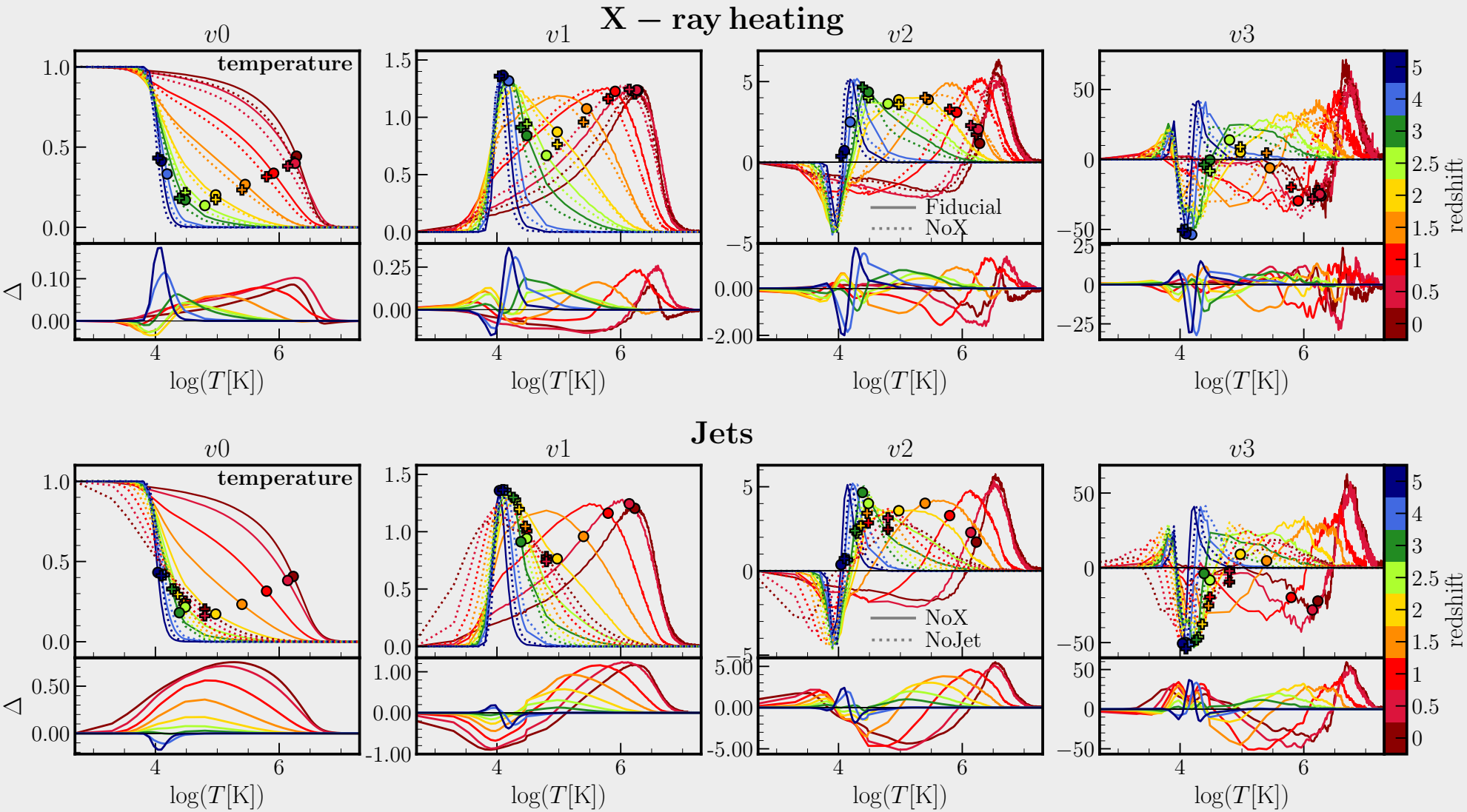
Temperature field



X-ray heating

- 2 epochs: $z > 4$ on cold (T $\simeq 10^4$K) gas (heating or removal of cold gas)
  $z < 1.5$ on hot (T $\gtrsim 10^5$K) gas (enabling jet feedback to be more effective at redistributing baryons into IGM)

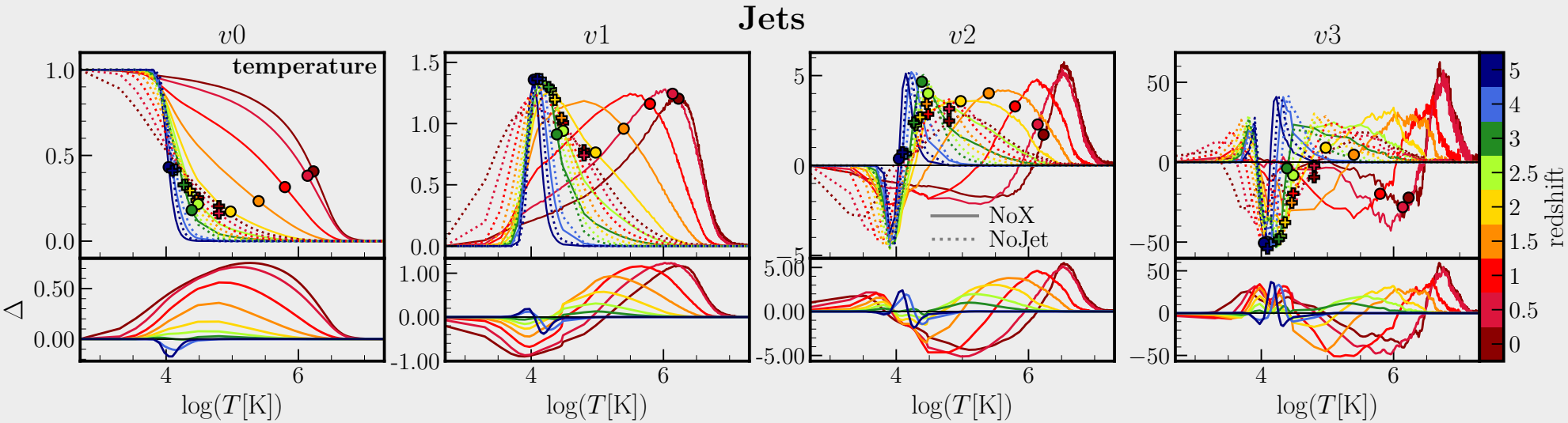
Temperature field



Temperature field

AGN jets

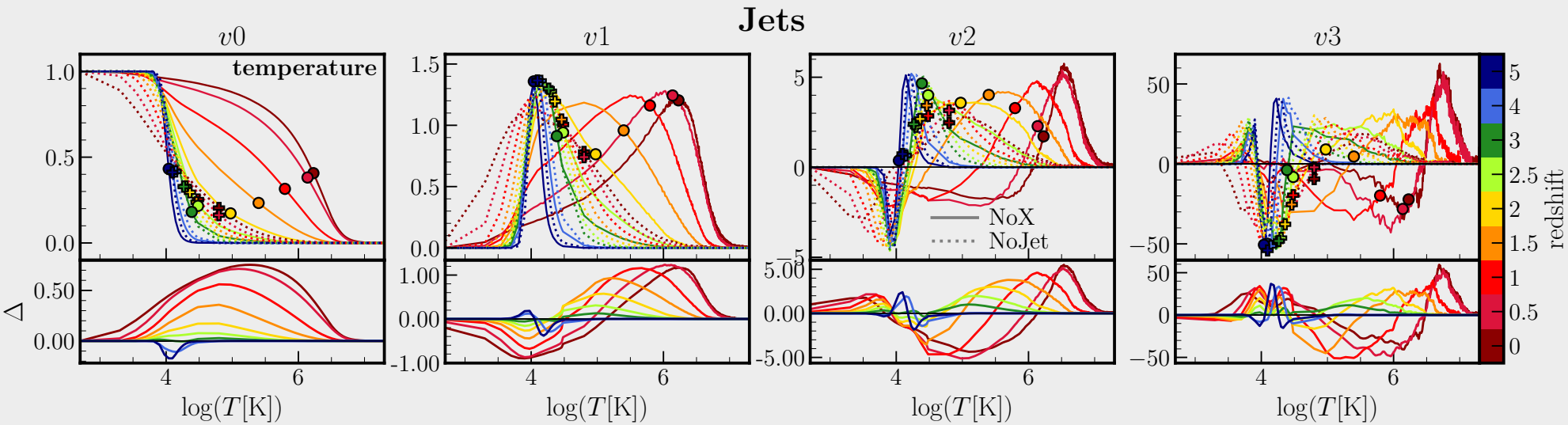
- strongest impact on the morphology of the T-field at $z \lesssim 2$



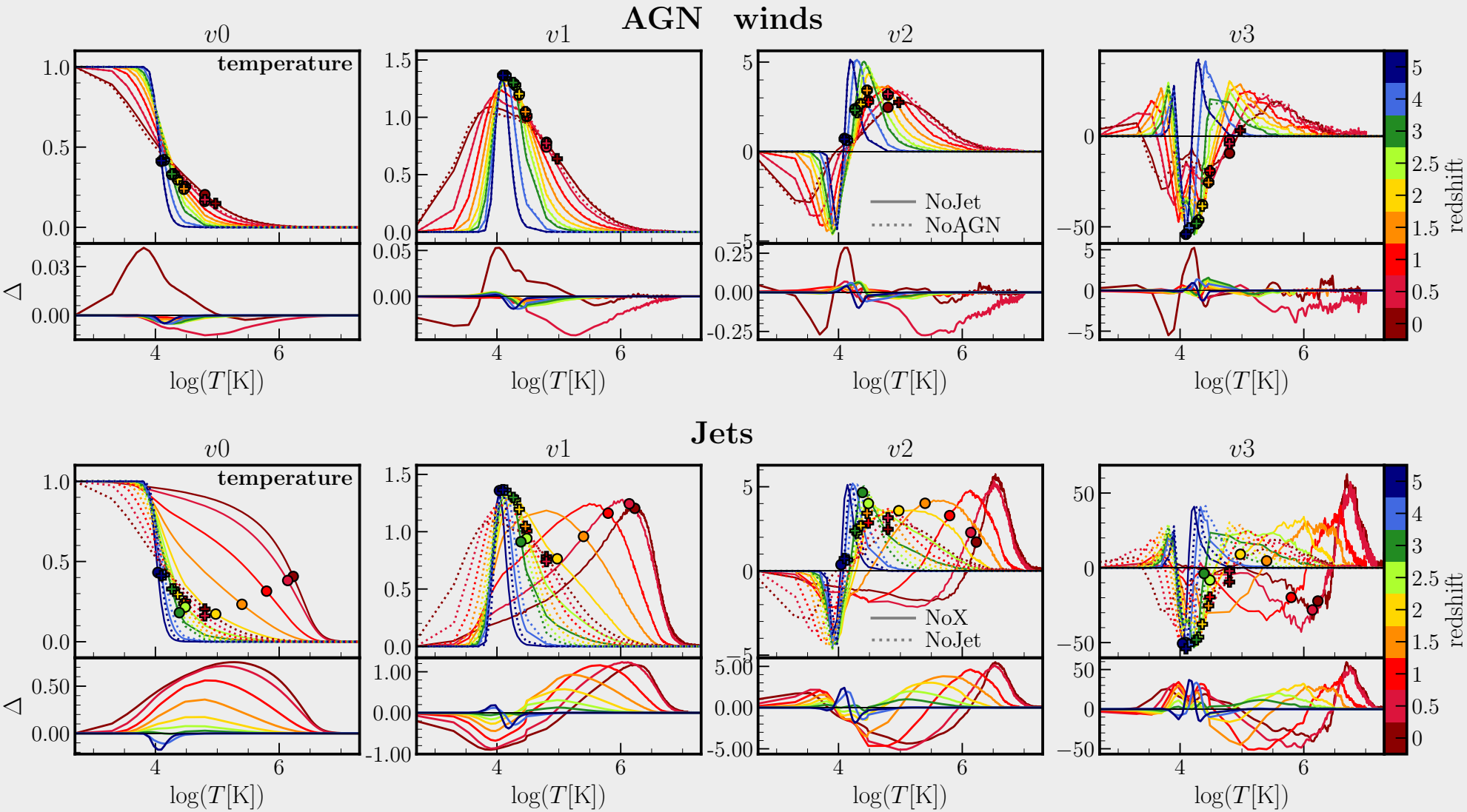
Temperature field

AGN jets

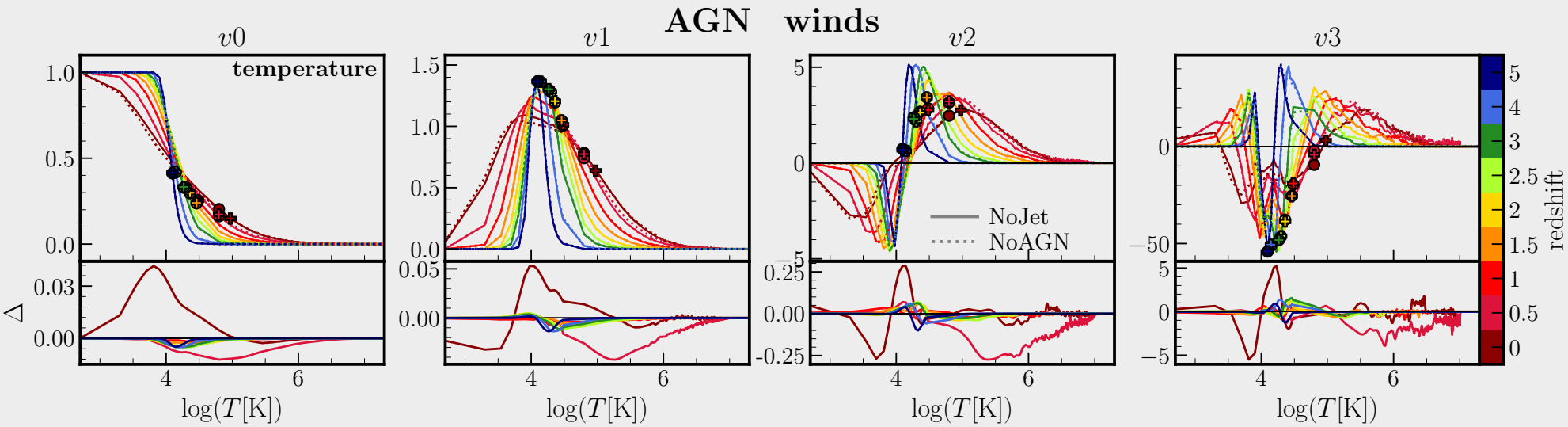
- strongest impact on the morphology of the T-field at $z \lesssim 2$
- v0: increase by more than 50% (T $> 10^4$K)
- v1: skew by decreasing (increasing) v1 of cold (hot) regions
- v2: almost reverse the convexity of T $> 10^4$K regions
- v3: alter the relative abundance of clumps, tunnels and bubbles



Temperature field



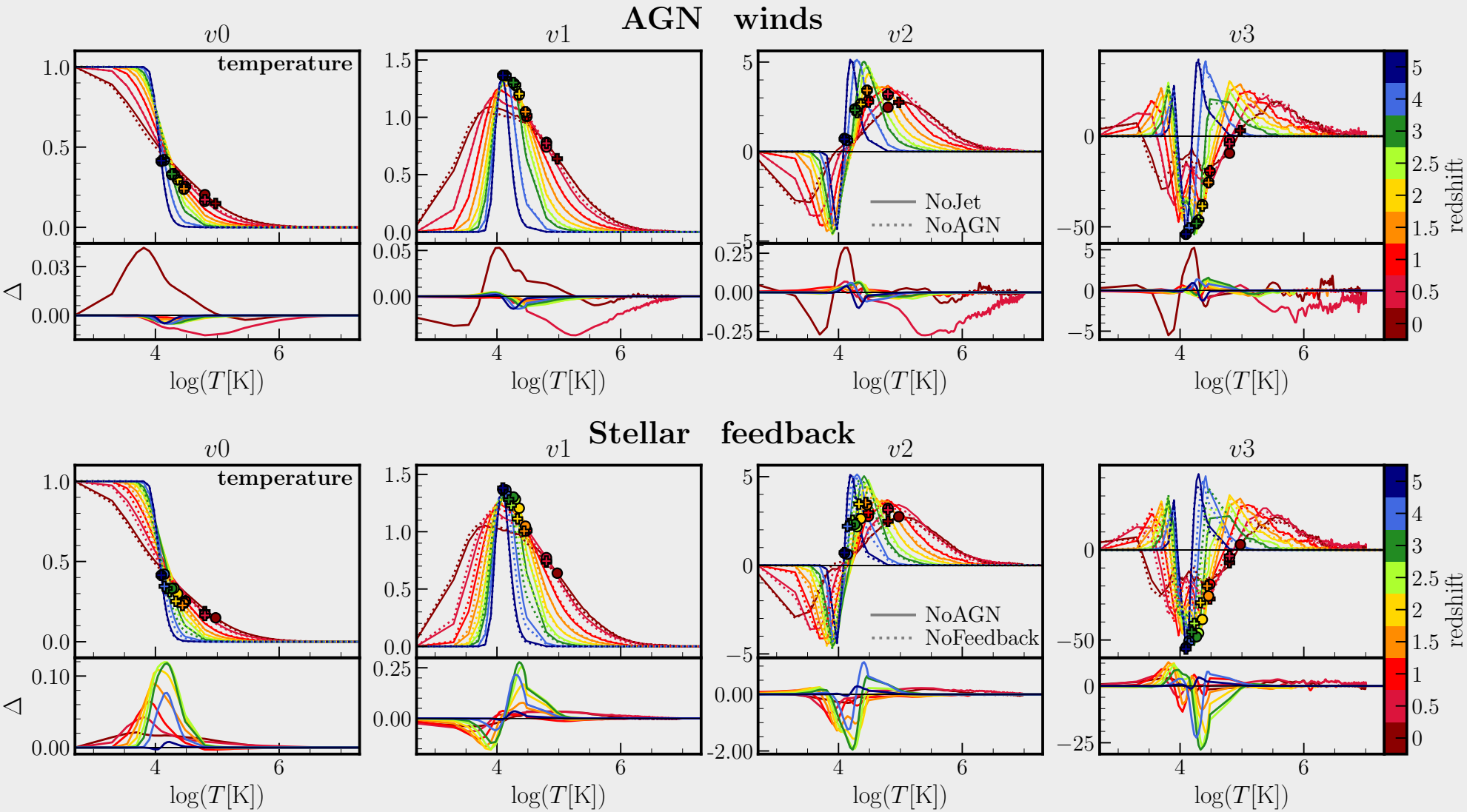
Temperature field



AGN winds

- smallest impact on the morphology of the T-field, limited to $z \lesssim 0.5$ for regions with T $\sim 10^{4.5} - 10^{5.5}$K

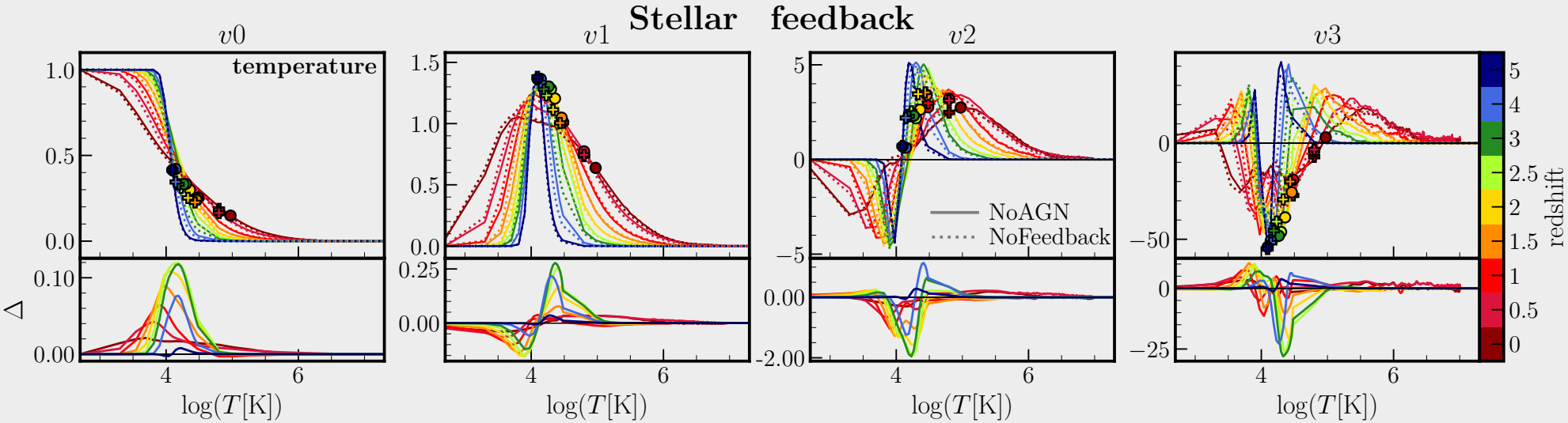
Temperature field



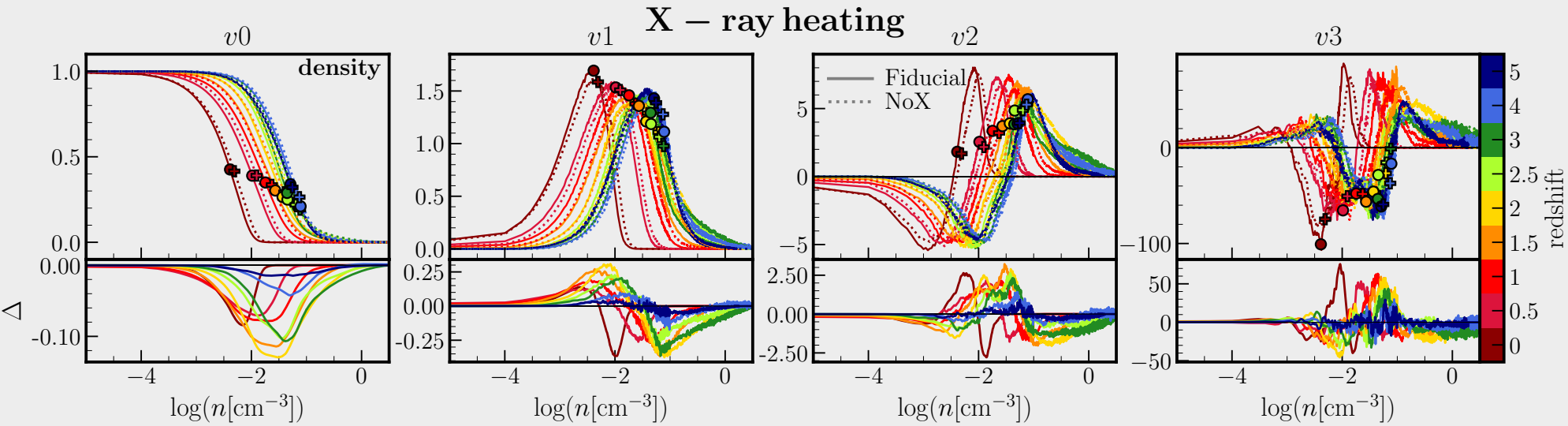
Temperature field

No feedback

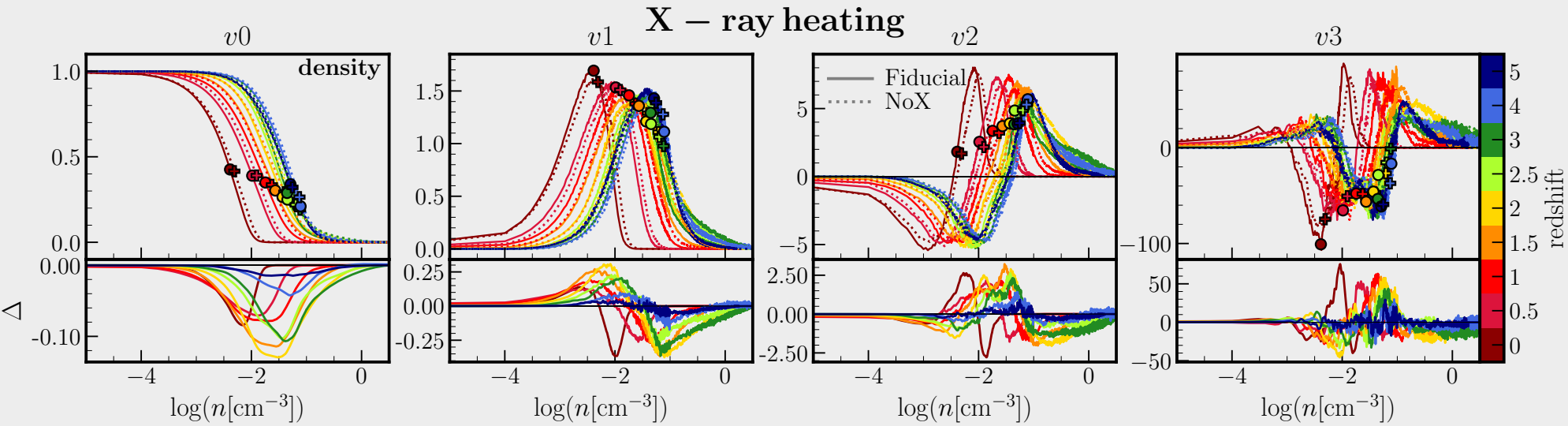
- regions with T $\gtrsim 10^4$K (besides small deviations at $z < 0.5$)
  - v0: fill about 1/3 of volume
  - v1: have maximum surface density
  - v2: have vanishing mean curvature
  - v3: have minimum (negative) Euler characteristic (network of cold filaments set by pure gravity and hydrodynamics)



Density field



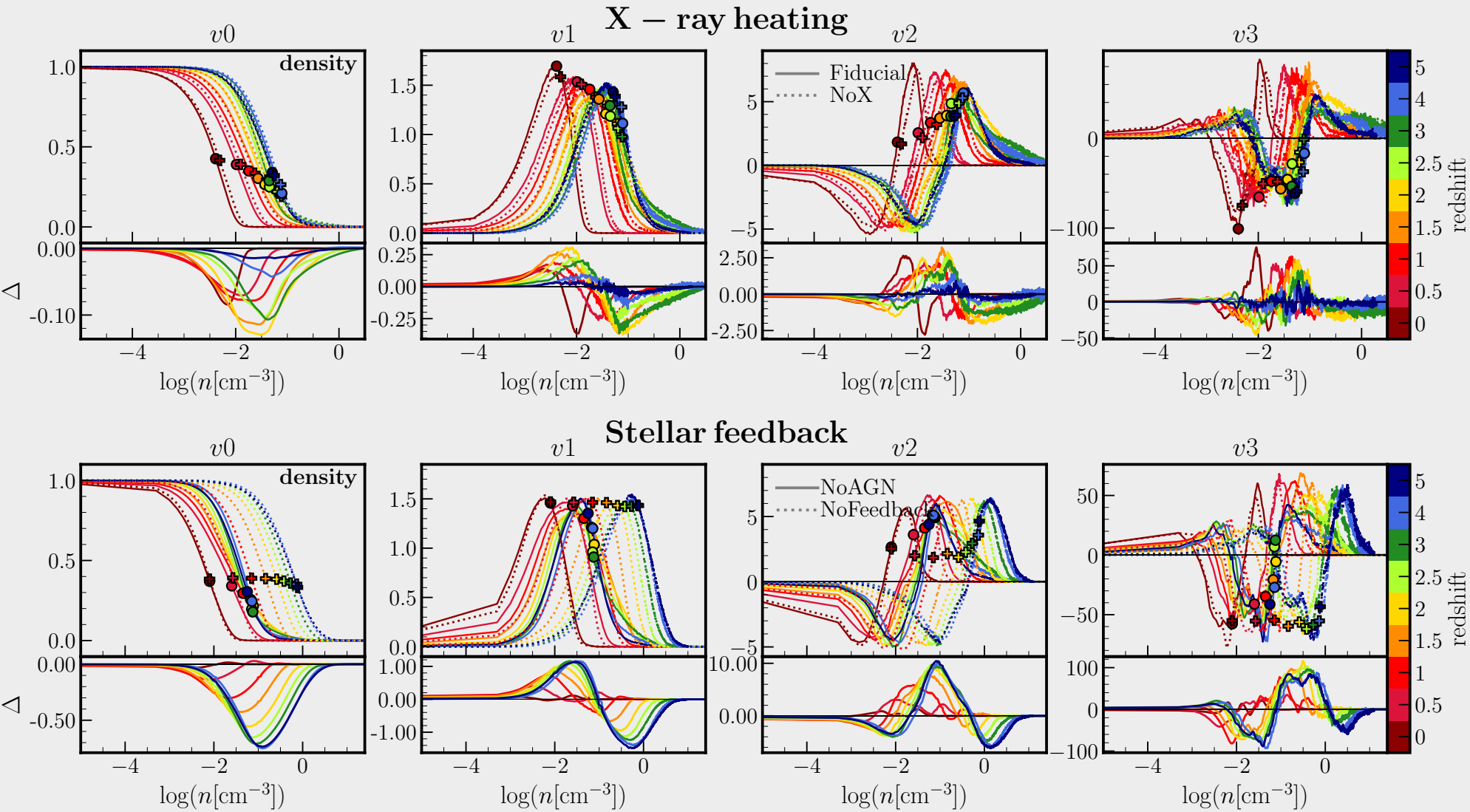
Density field



All feedbacks

- v0: domains with mean density $\bar{\mathrm{n}}$ occupy increasing fraction of volume from 20% to 40% from $z = 5 - 0$
- v1 & v2: $z \lesssim 2$ $\bar{\mathrm{n}}$-domains have largest surface area & decreasing convexity (v2 > 0)
- v3: network of tunnels defined by $\bar{\mathrm{n}}$-regions already in place at $z = 5$, grows until $z \sim 3$, grows again at $z \lesssim 1$ at the expense of higher density clumps occupying a tiny fraction of the total volume

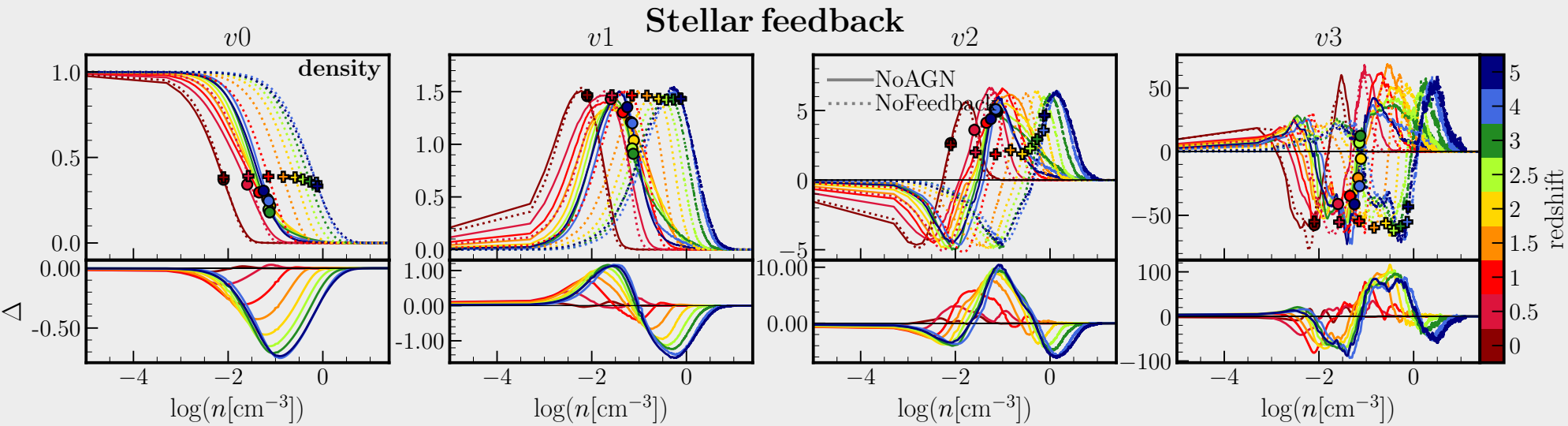
Density field



Density field

Stellar feedback

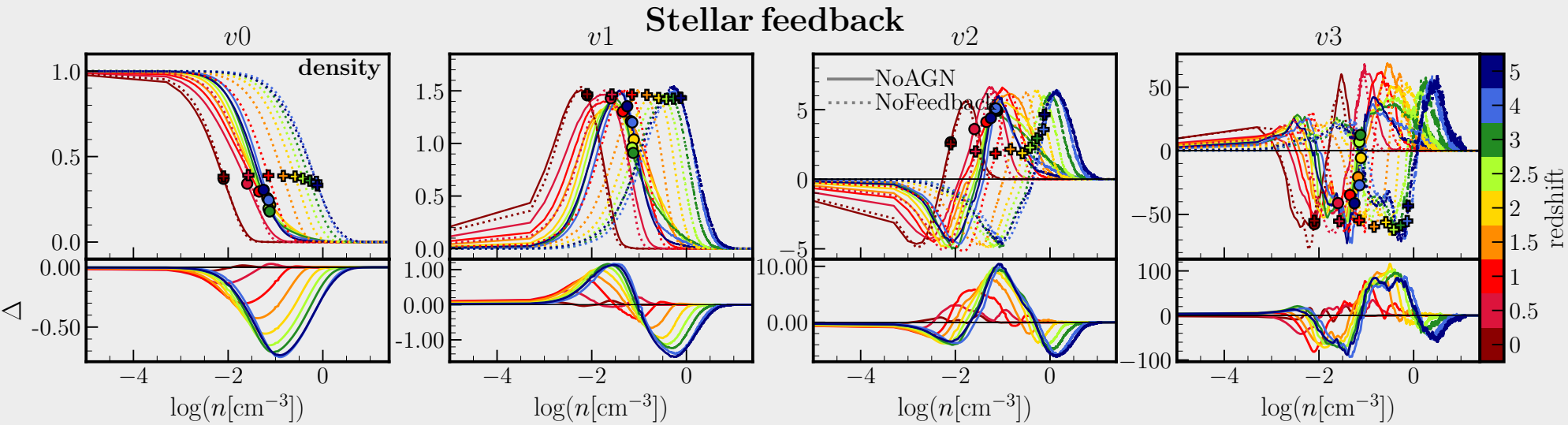
- largest impact on the morphology of the density field



Density field

Stellar feedback

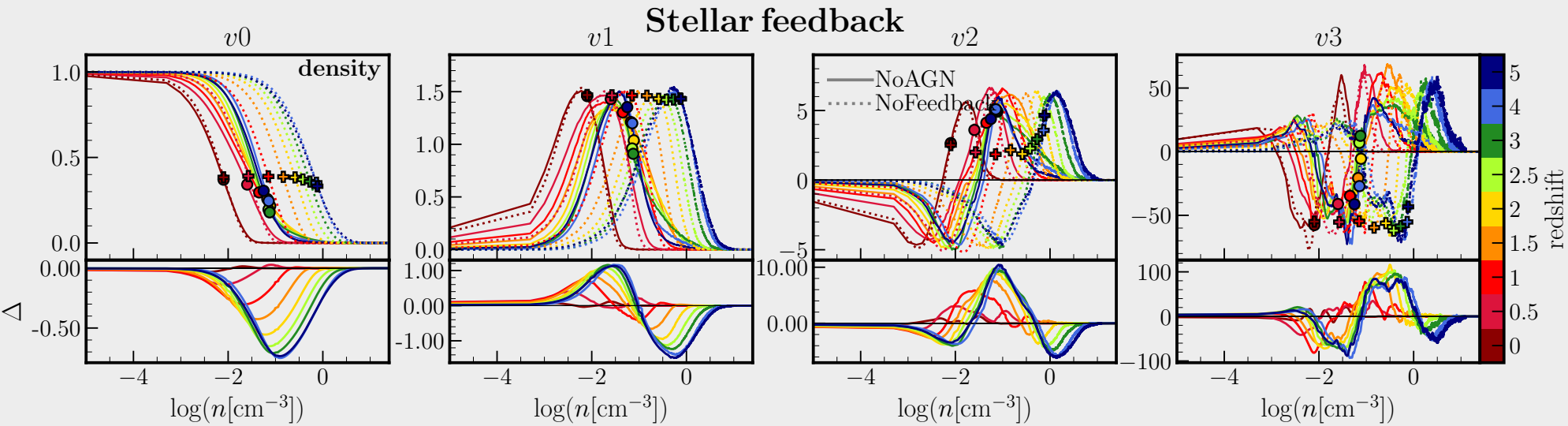
- largest impact on the morphology of the density field
- no feedback: smoothing evolution down to $z = 0$; for all but v2, MFs of $\bar{n}$-regions are constant over time; global topology dominated by tunnels



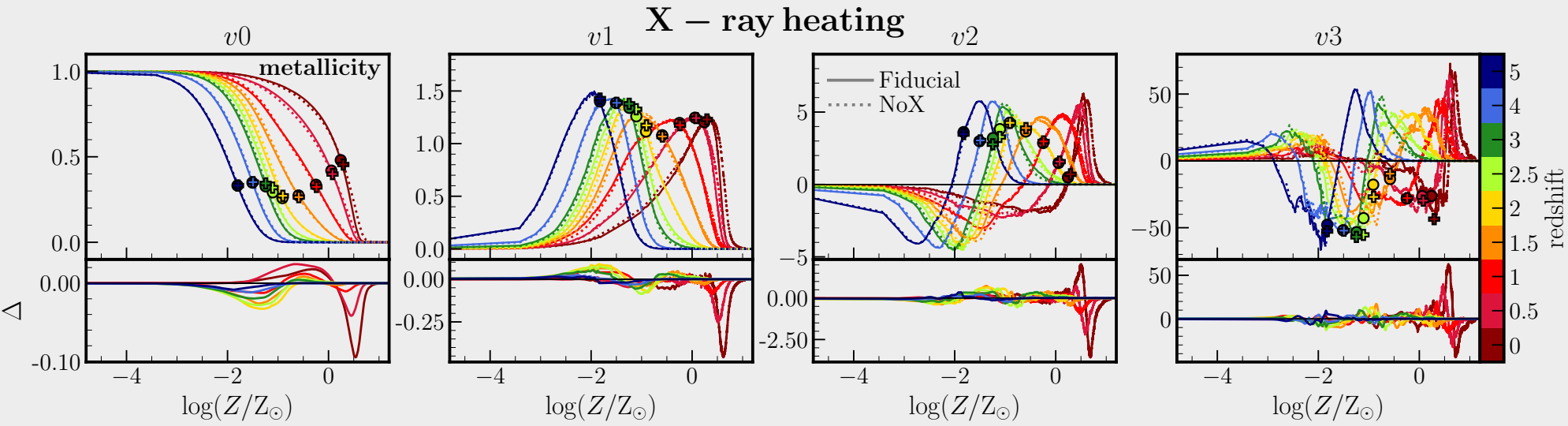
Density field

Stellar feedback

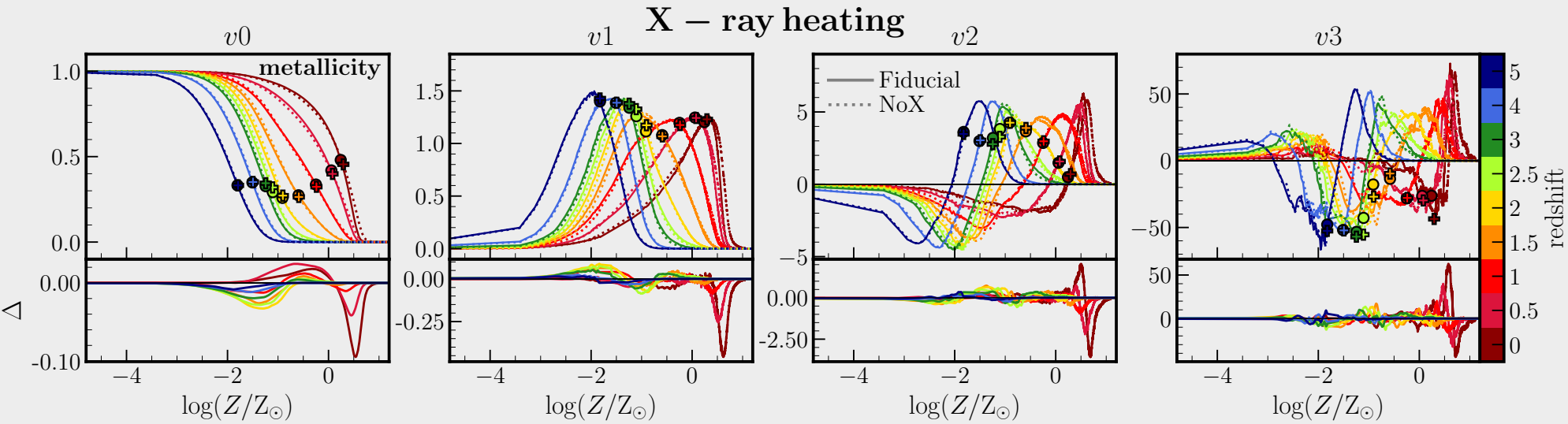
- largest impact on the morphology of the density field
- no feedback: smoothing evolution down to $z = 0$; for all but v2, MFs of $\bar{n}$-regions are constant over time; global topology dominated by tunnels
- stellar feedback: time evolution of $\bar{n}$-regions is halted until $z \sim 1.5$ (late-end of the SFR peak)
  : at $z > 2$ - limits the abundance and size of gas regions to lower values; reduces the number of tunnels; but doesn't modify the convexity
  : at $z < 1$ - morphologically not efficient anymore



Metallicity field



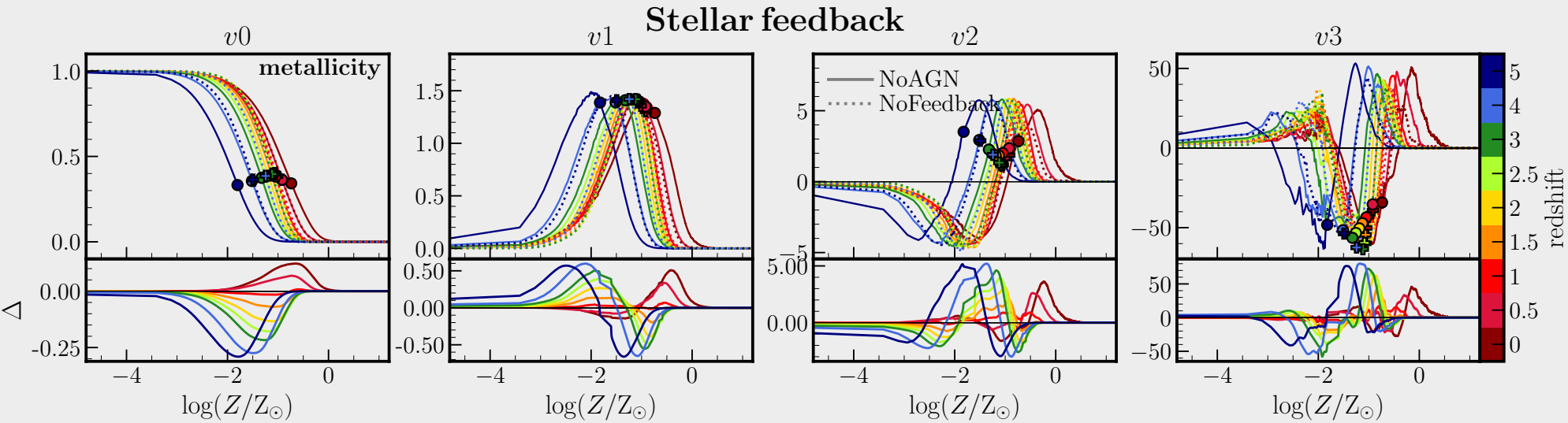
Metallicity field



All feedbacks

- redshift evolution similar to T-field, different from n-field: global metal enrichment over time
- v0: growth of mean metallicity with time, $\bar{Z}$-domains expand strongly after $z \sim 1.5$, up to 50% at z=0
- v1: surface density of metal poor (rich) regions decreases (increases) with time
- v2 & v3: positive for metal rich ($\gtrsim 1.8$ $Z_\odot$) regions (network of sparse metal-rich clumps)

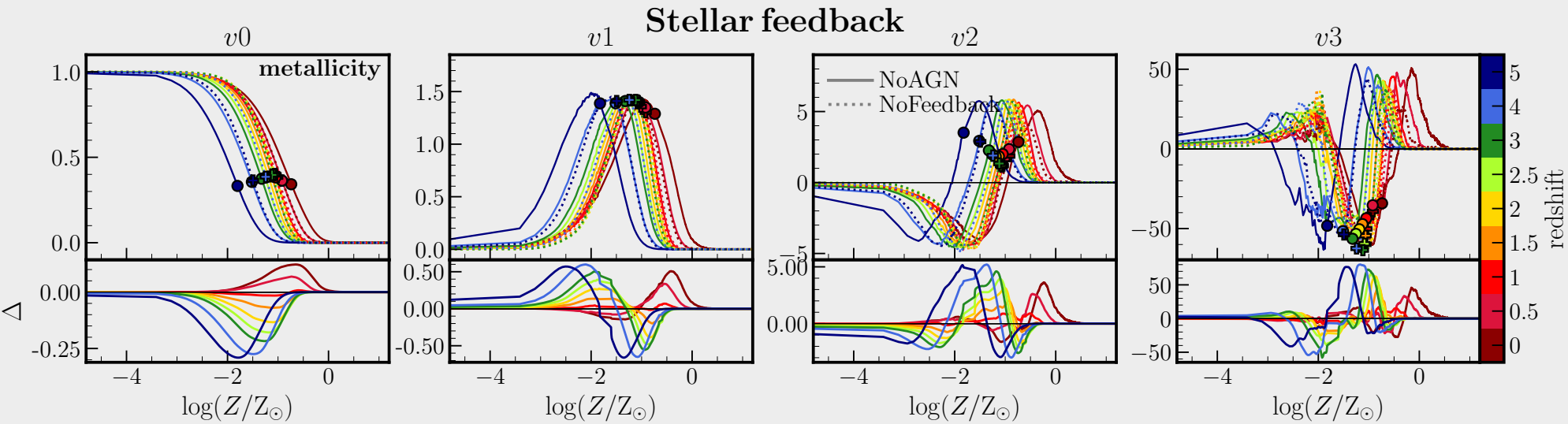
Metallicity field



Metallicity field

Stellar feedback

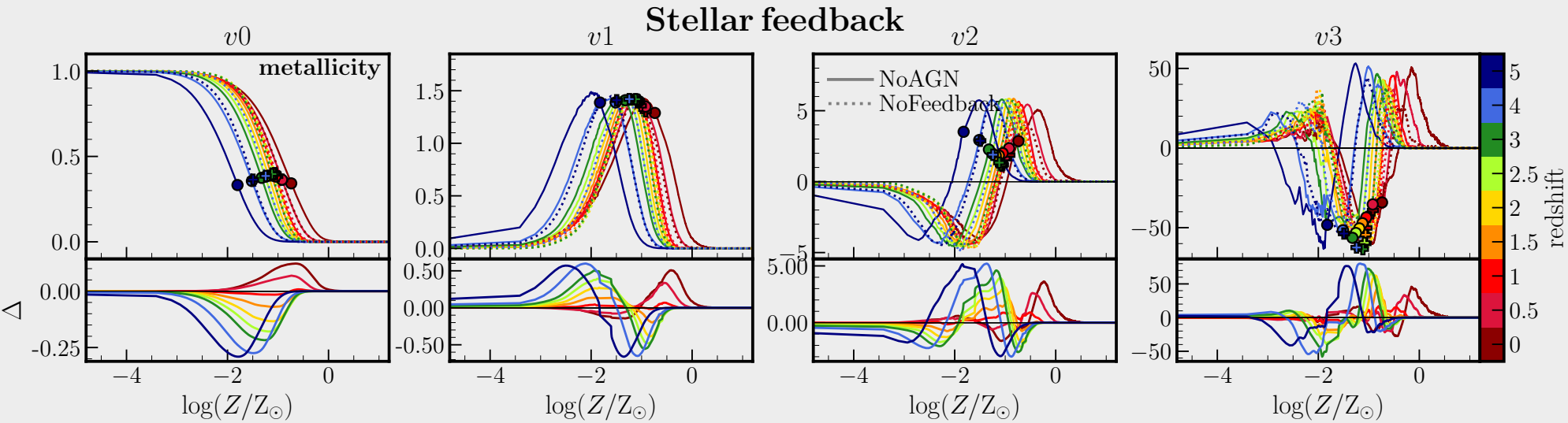
- at $z > 1.5$ morphology of Z-field is strongly impacted by stellar feedback ($Z \lesssim 0.1\ Z_\odot$)
- v0: reduced by 5-25%
- v1 & v2: substantially altered



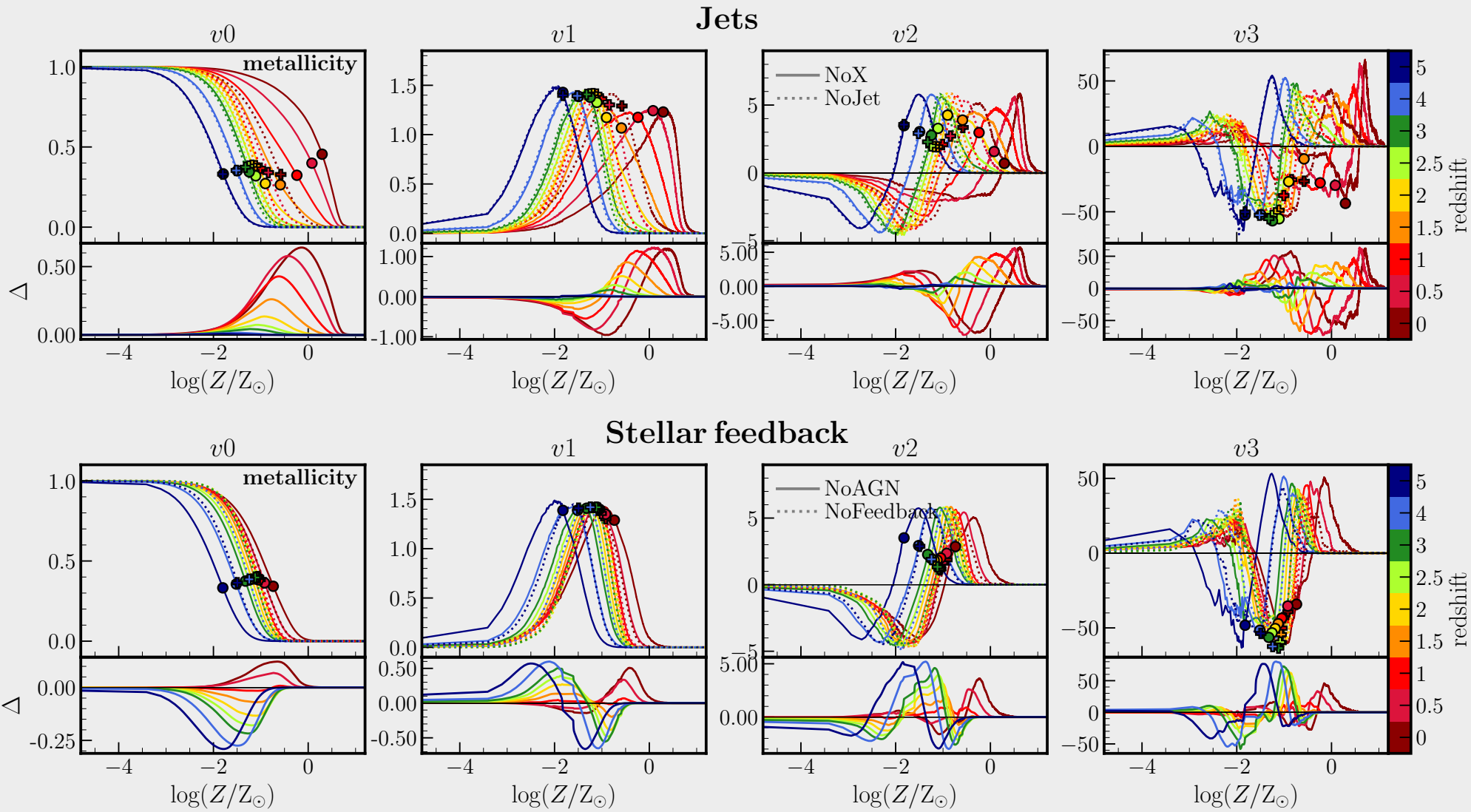
Metallicity field

Stellar feedback

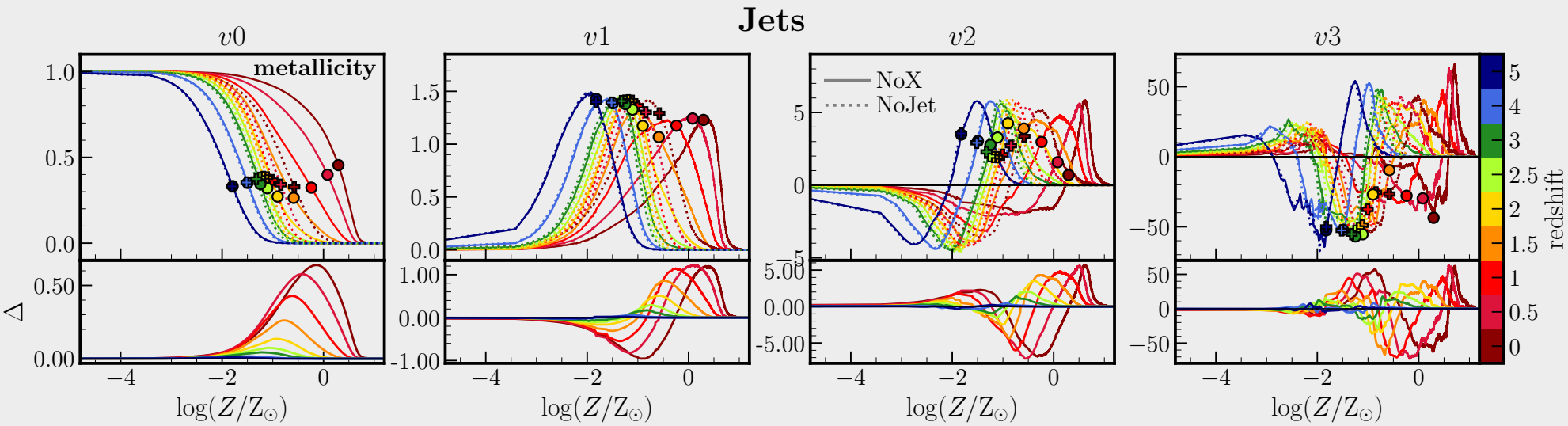
- at $z > 1.5$ morphology of Z-field is strongly impacted by stellar feedback (Z $\lesssim 0.1$ $Z_\odot$)
- v0: reduced by 5-25%
- v1 & v2: substantially altered
- at $z < 1.5$ impacts morphology of regions Z > 0.01 $Z_\odot$ (especially Z ~ 0.1 $Z_\odot$) with AGN feedback (especially AGN jets)



Metallicity field



Metallicity field



AGN jets

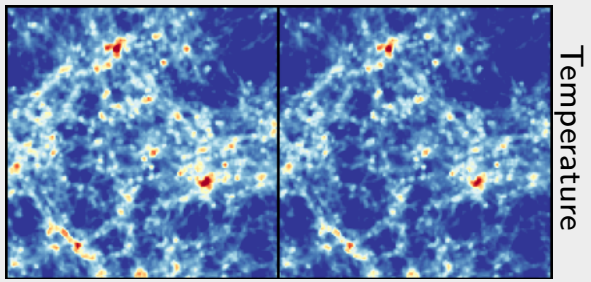
- play major role at $z < 1.5$
- v0: increase by up to 60% at $z = 0$
- v1: decrease (increase) for low (high) metallicity regions
- v2 & v3: change the mean curvature and topology (enhancing metal-rich regions)

Ranking of feedback mechanisms

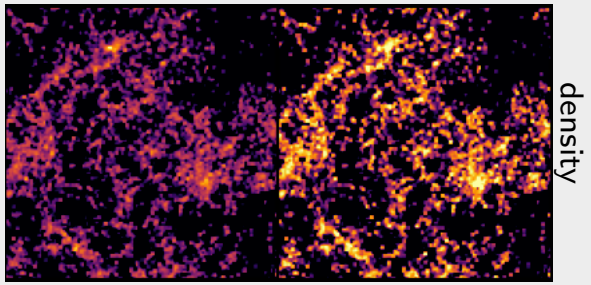
	T	P	n	$n_{\rm HI}$	$n_{\rm H_2}$	Z
X-ray heating	2	2	2	2	2	4
Jets	1	3	3	3	3	2
AGN winds	4	4	4	4	4	3
Stellar feedback	3	1	1	1	1	1

$z \gtrsim 1.5$

Effect of Jets



Effect of Stellar feedback



Ranking of feedback mechanisms

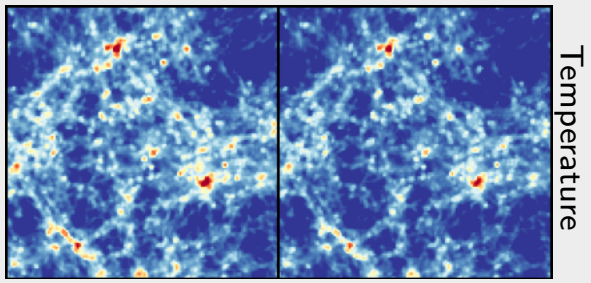
	T	P	n	$n_{\rm HI}$	$n_{\rm H_2}$	Z
X-ray heating	2	2	2	2	2	4
Jets	1	3	3	3	3	2
AGN winds	4	4	4	4	4	3
Stellar feedback	3	1	1	1	1	1

$z \gtrsim 1.5$

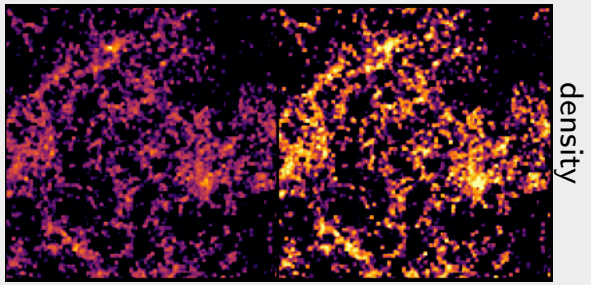
	T	P	n	$n_{\rm HI}$	$n_{\rm H_2}$	Z
X-ray heating	2	3	4	2	4	3
Jets	1	2	3	4	3	1
AGN winds	4	1	2	3	2	4
Stellar feedback	3	1	1	1	1	2

$z \lesssim 1.5$

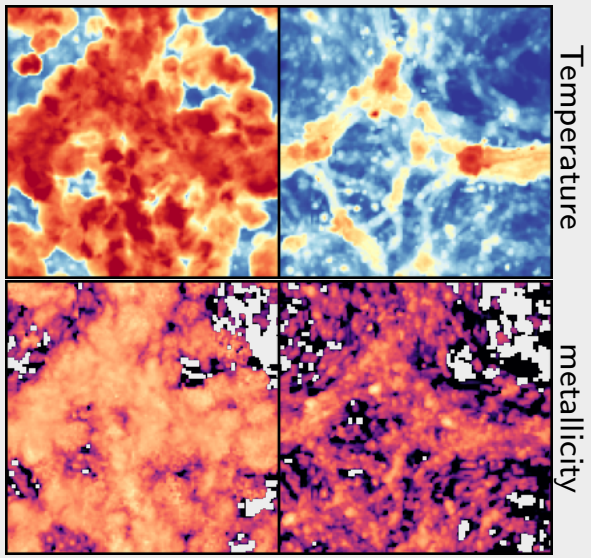
Effect of Jets



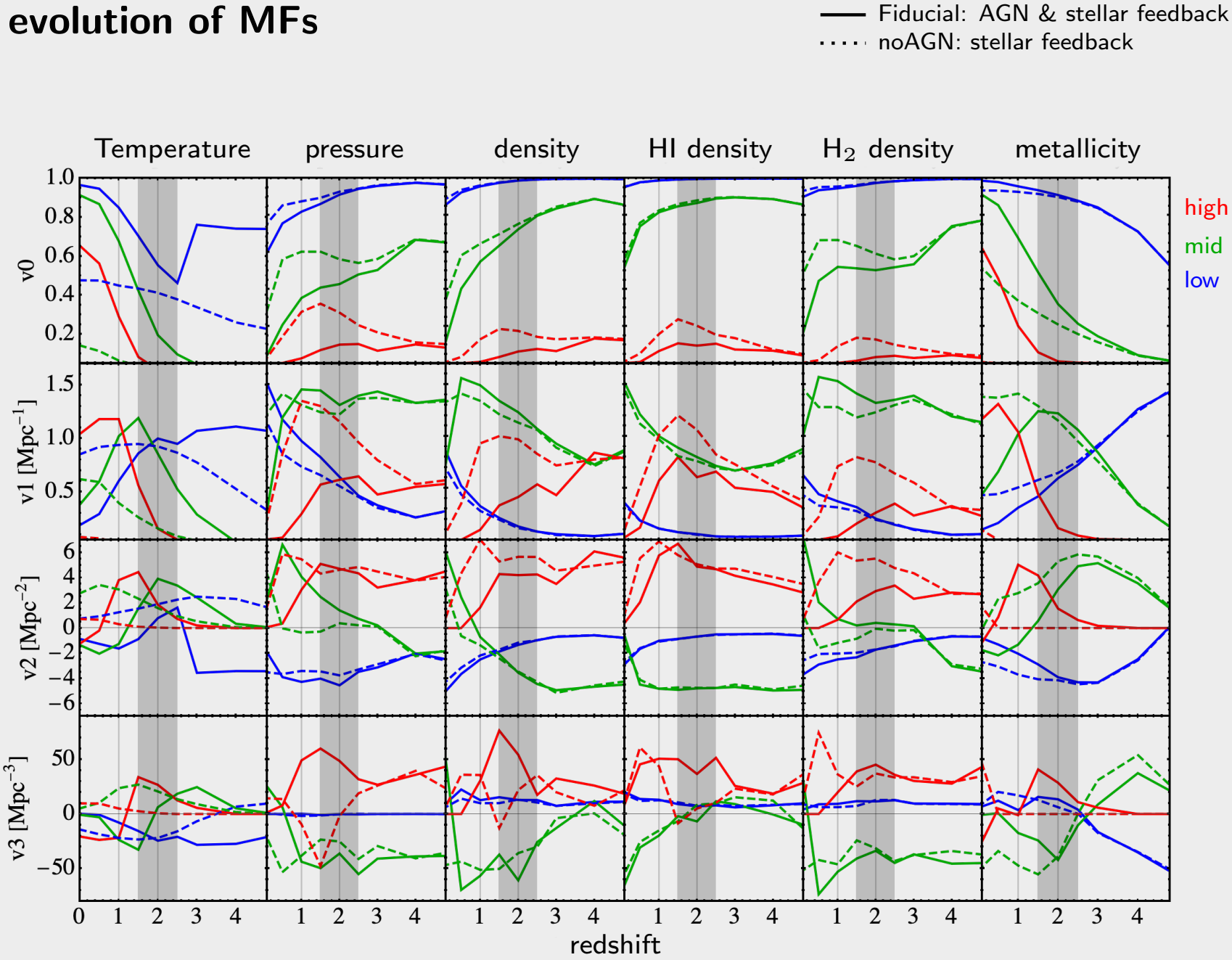
Effect of Stellar feedback



Effect of Jets

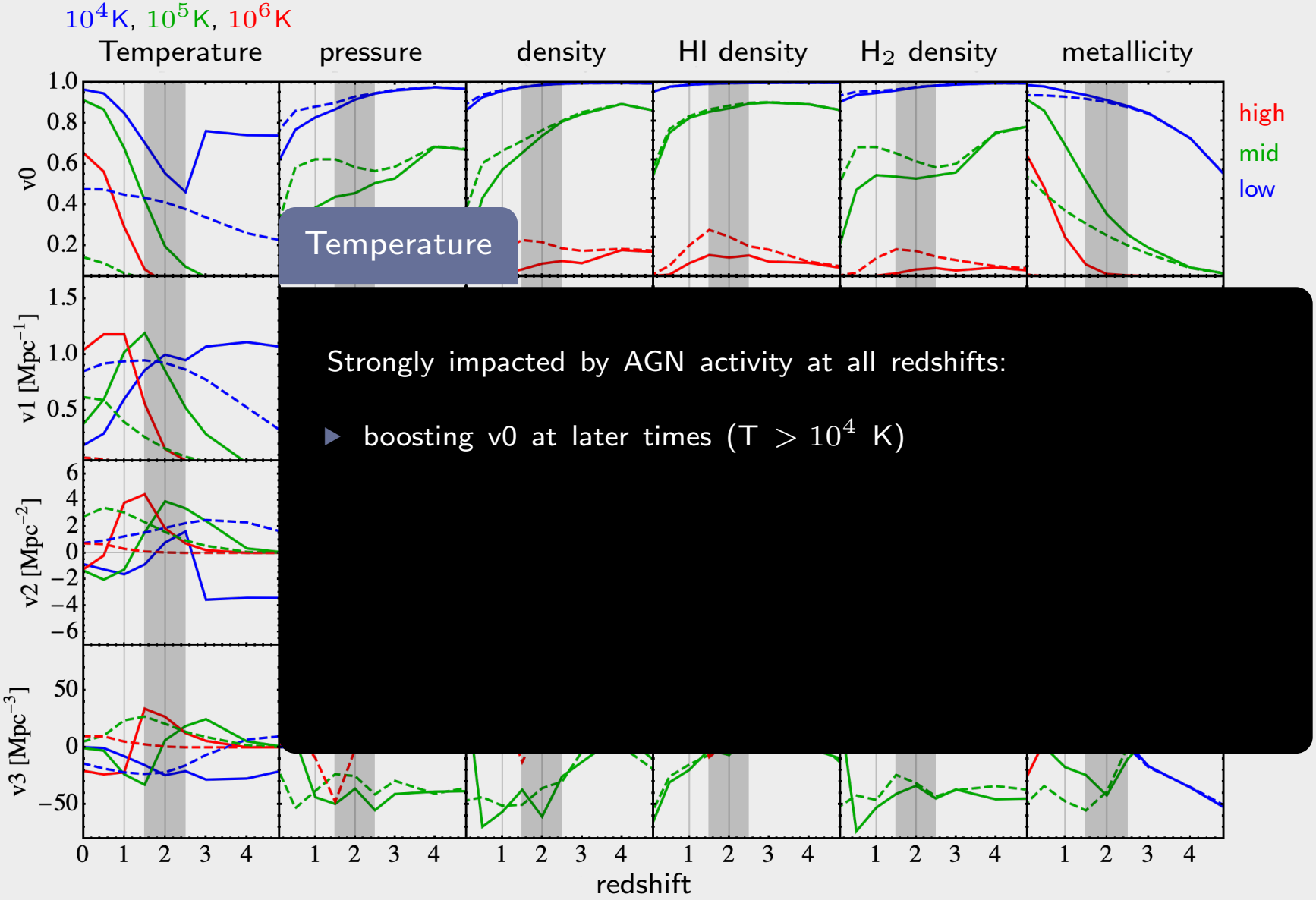


Time evolution of MFs



Time evolution of MFs

Fiducial: AGN & stellar feedback
noAGN: stellar feedback



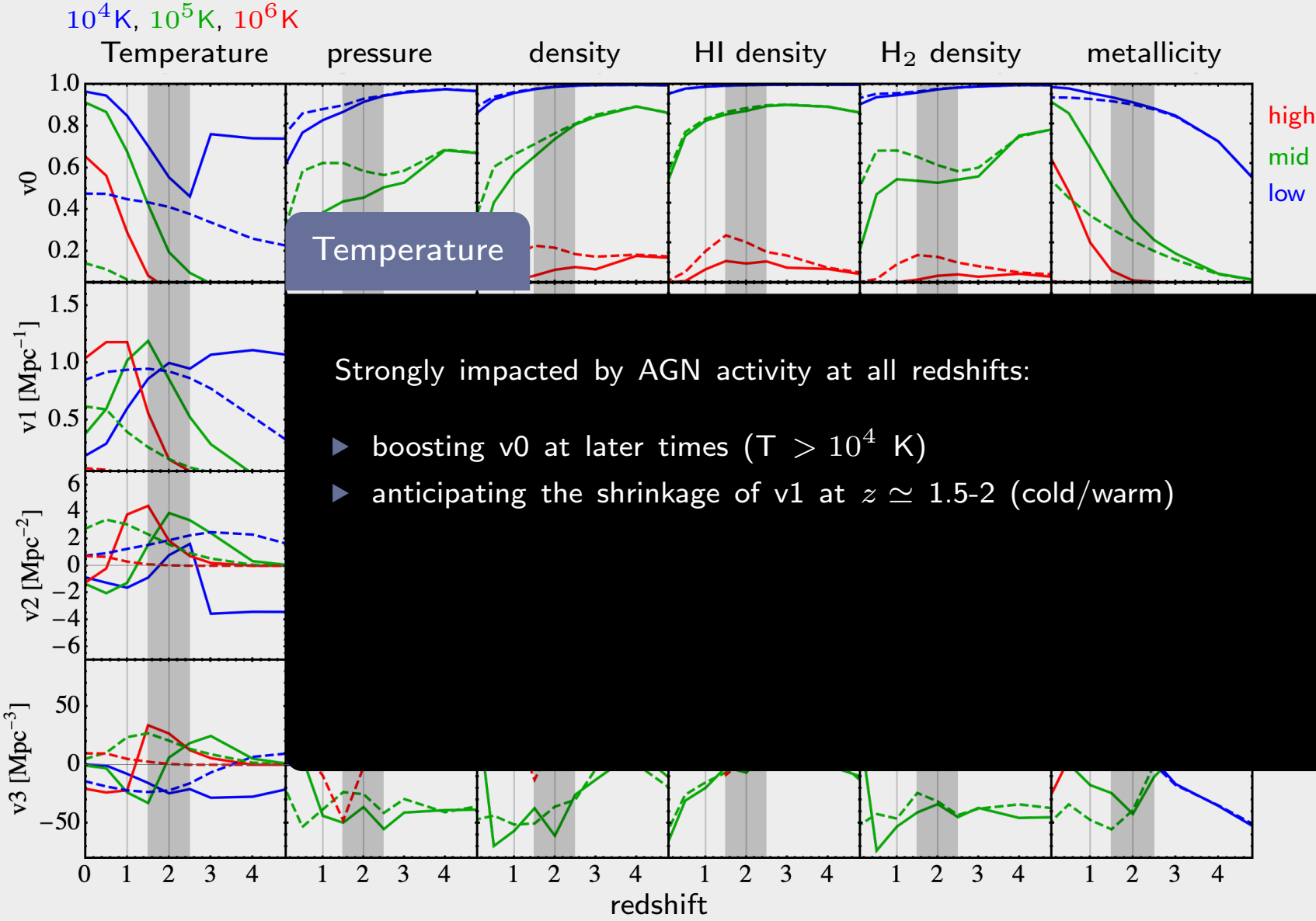
Temperature

Strongly impacted by AGN activity at all redshifts:

- boosting v0 at later times (T $> 10^4$ K)

Time evolution of MFs

Fiducial: AGN & stellar feedback
noAGN: stellar feedback



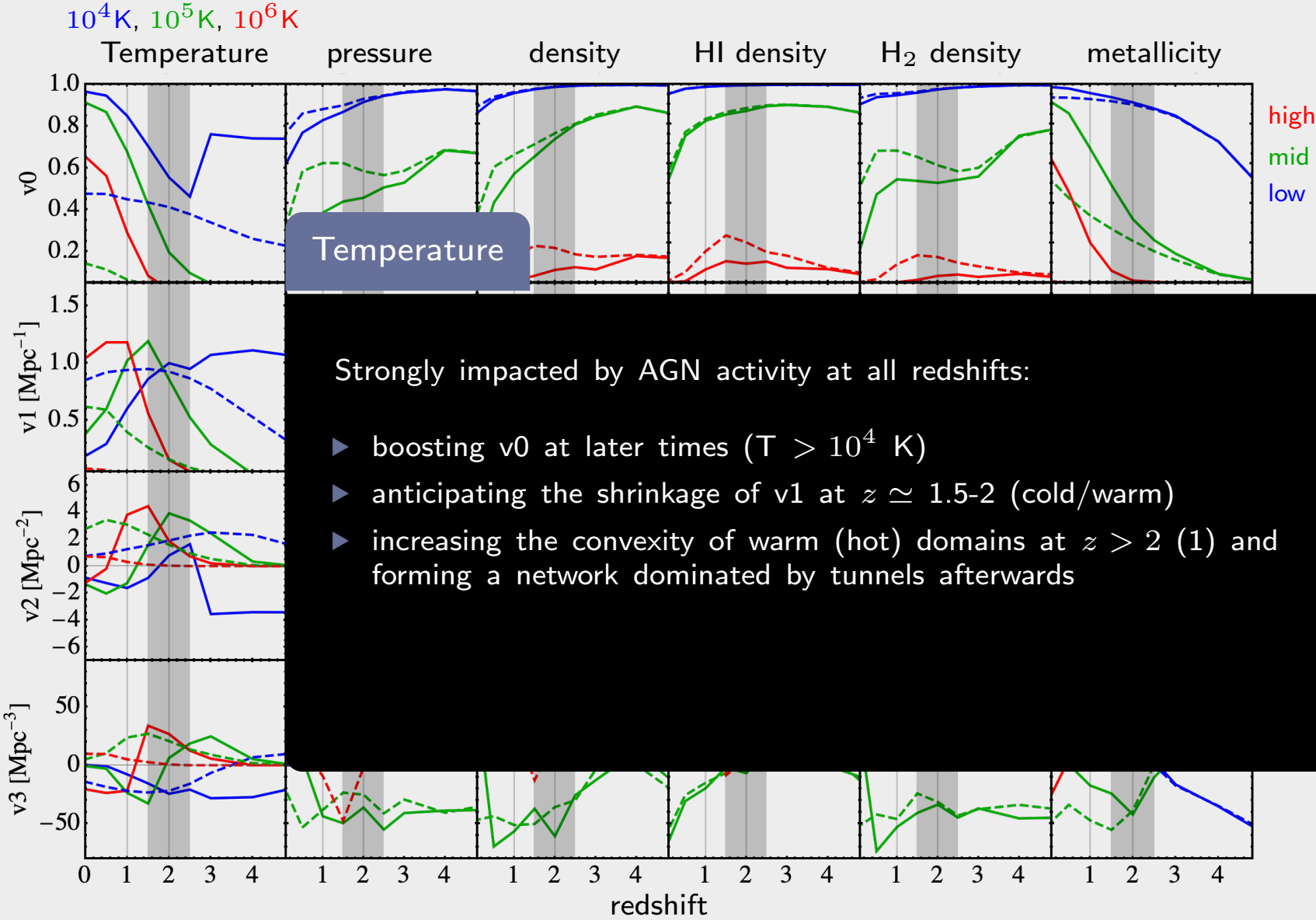
Temperature

Strongly impacted by AGN activity at all redshifts:

- boosting v0 at later times (T $> 10^4$ K)
- anticipating the shrinkage of v1 at $z \simeq$ 1.5-2 (cold/warm)

Time evolution of MFs

Fiducial: AGN & stellar feedback
noAGN: stellar feedback



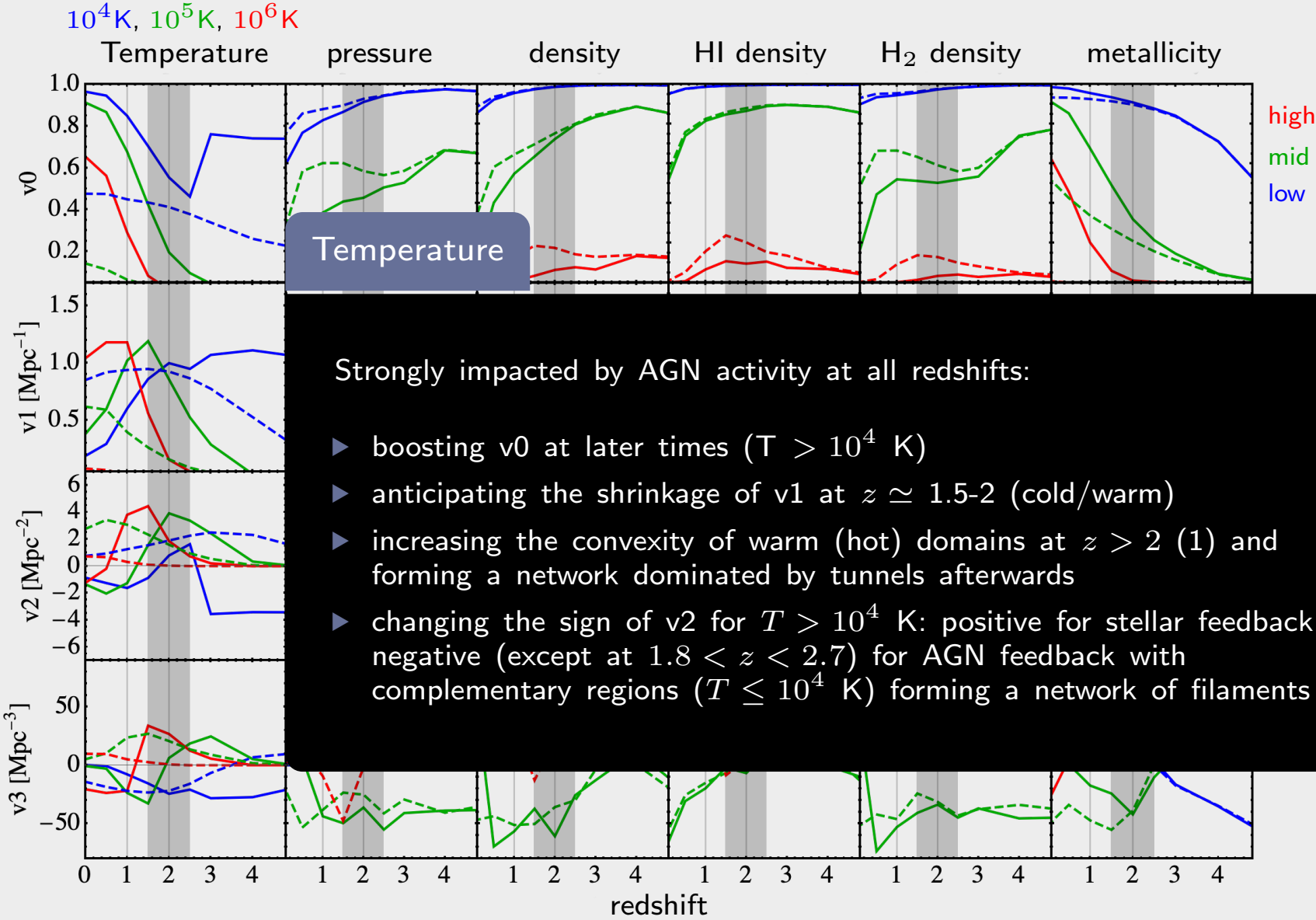
Temperature

Strongly impacted by AGN activity at all redshifts:

- boosting v0 at later times (T $> 10^4$ K)
- anticipating the shrinkage of v1 at $z \simeq$ 1.5-2 (cold/warm)
- increasing the convexity of warm (hot) domains at $z > 2$ (1) and forming a network dominated by tunnels afterwards

Time evolution of MFs

Fiducial: AGN & stellar feedback
noAGN: stellar feedback



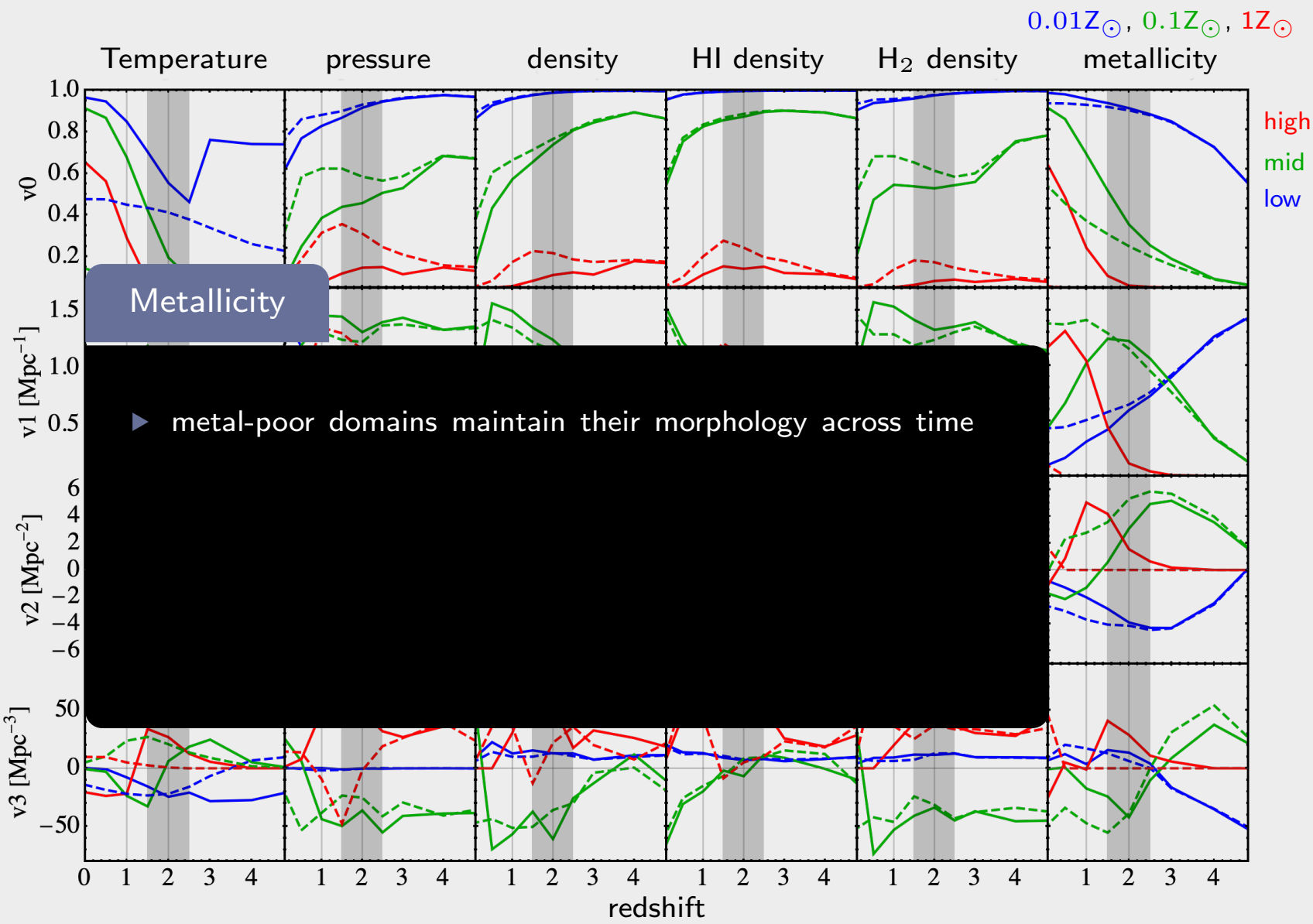
Temperature

Strongly impacted by AGN activity at all redshifts:

- boosting v0 at later times (T $> 10^4$ K)
- anticipating the shrinkage of v1 at $z \simeq$ 1.5-2 (cold/warm)
- increasing the convexity of warm (hot) domains at $z > 2$ (1) and forming a network dominated by tunnels afterwards
- changing the sign of v2 for $T > 10^4$ K: positive for stellar feedback; negative (except at $1.8 < z < 2.7$) for AGN feedback with complementary regions ($T \leq 10^4$ K) forming a network of filaments

Time evolution of MFs

Fiducial: AGN & stellar feedback
noAGN: stellar feedback

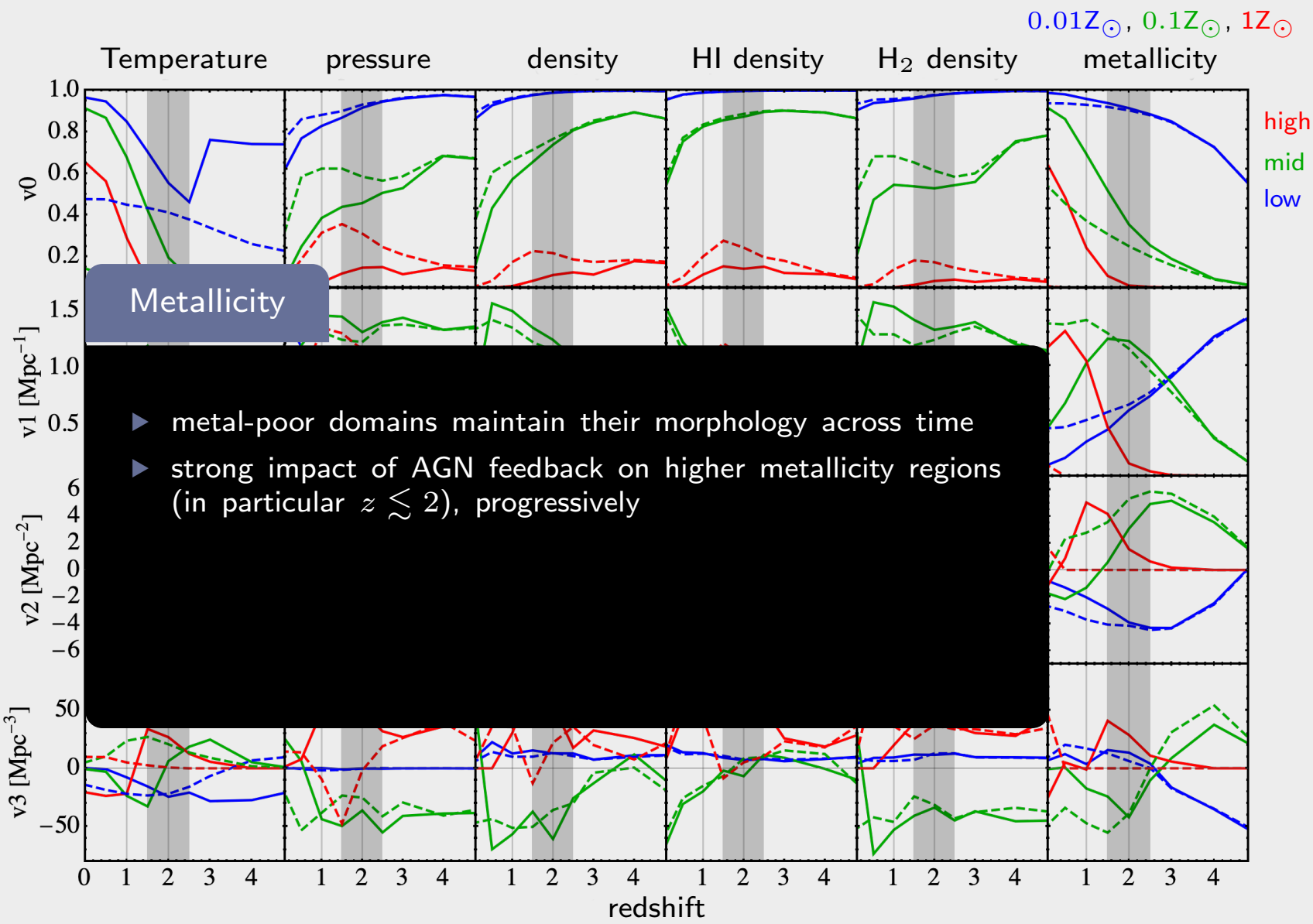


Metallicity

- metal-poor domains maintain their morphology across time

Time evolution of MFs

Fiducial: AGN & stellar feedback
noAGN: stellar feedback

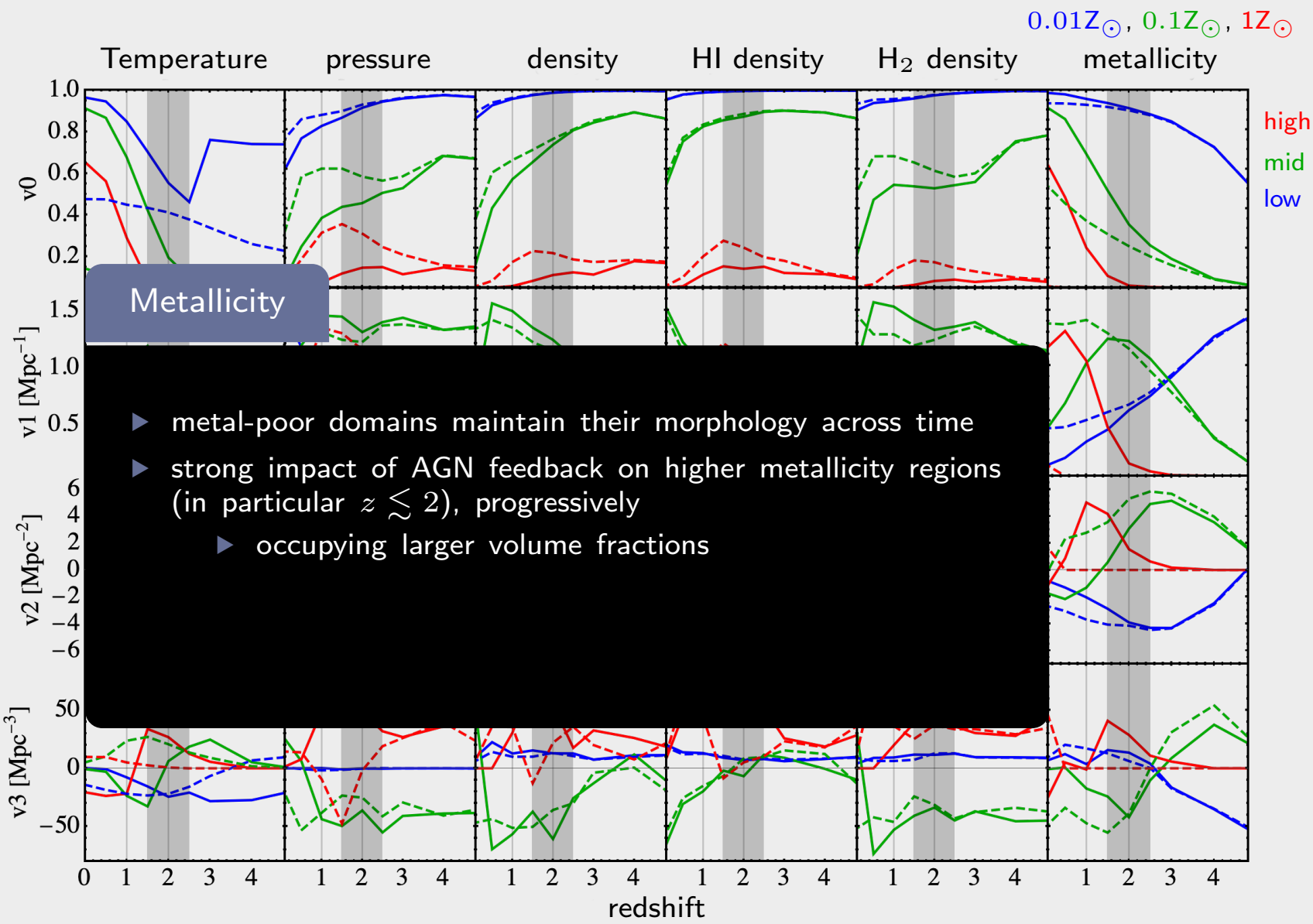


Metallicity

- metal-poor domains maintain their morphology across time
- strong impact of AGN feedback on higher metallicity regions (in particular $z \lesssim 2$), progressively

Time evolution of MFs

Fiducial: AGN & stellar feedback
noAGN: stellar feedback

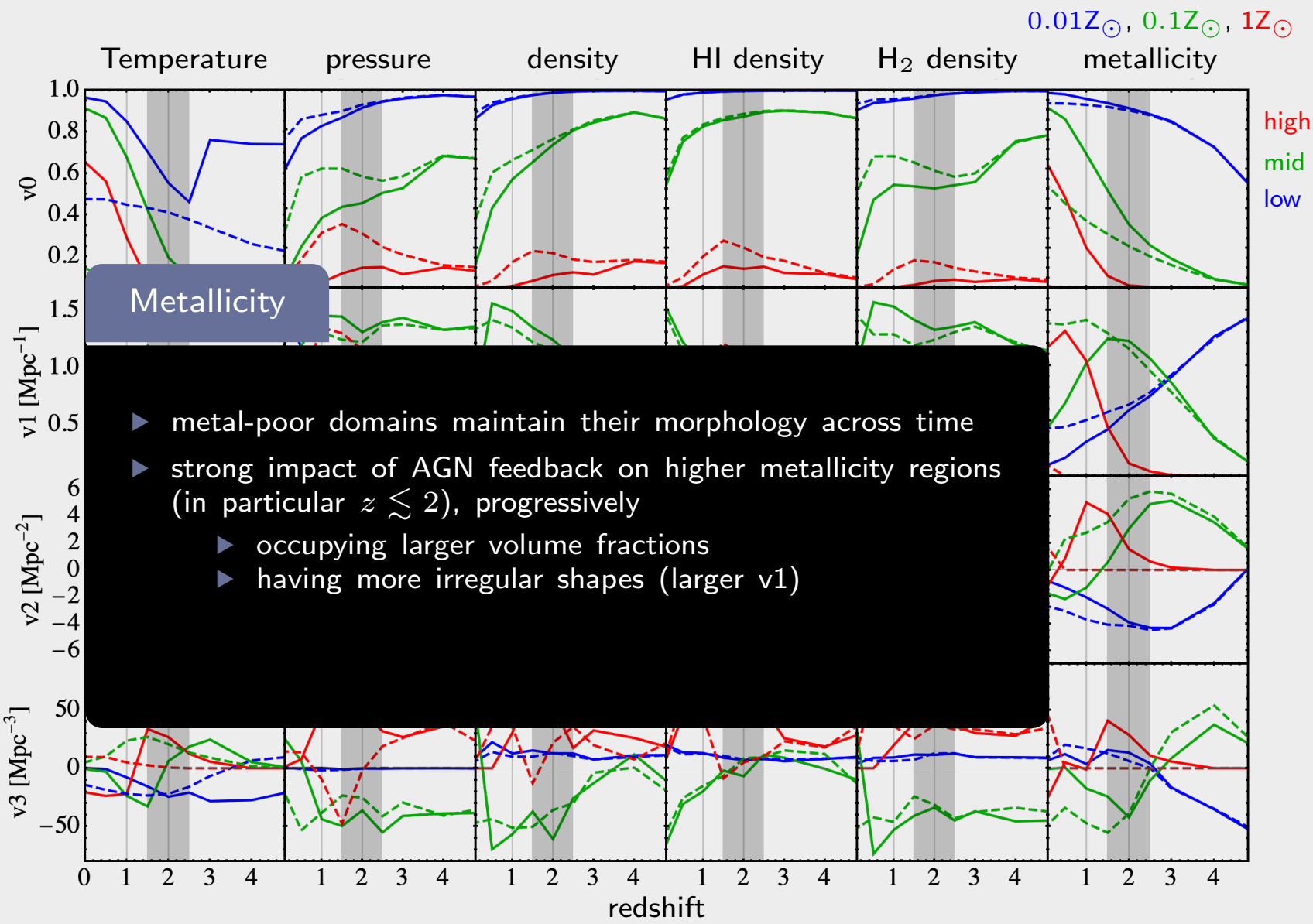


Metallicity

- metal-poor domains maintain their morphology across time
- strong impact of AGN feedback on higher metallicity regions (in particular $z \lesssim 2$), progressively
  - occupying larger volume fractions

Time evolution of MFs

Fiducial: AGN & stellar feedback
noAGN: stellar feedback

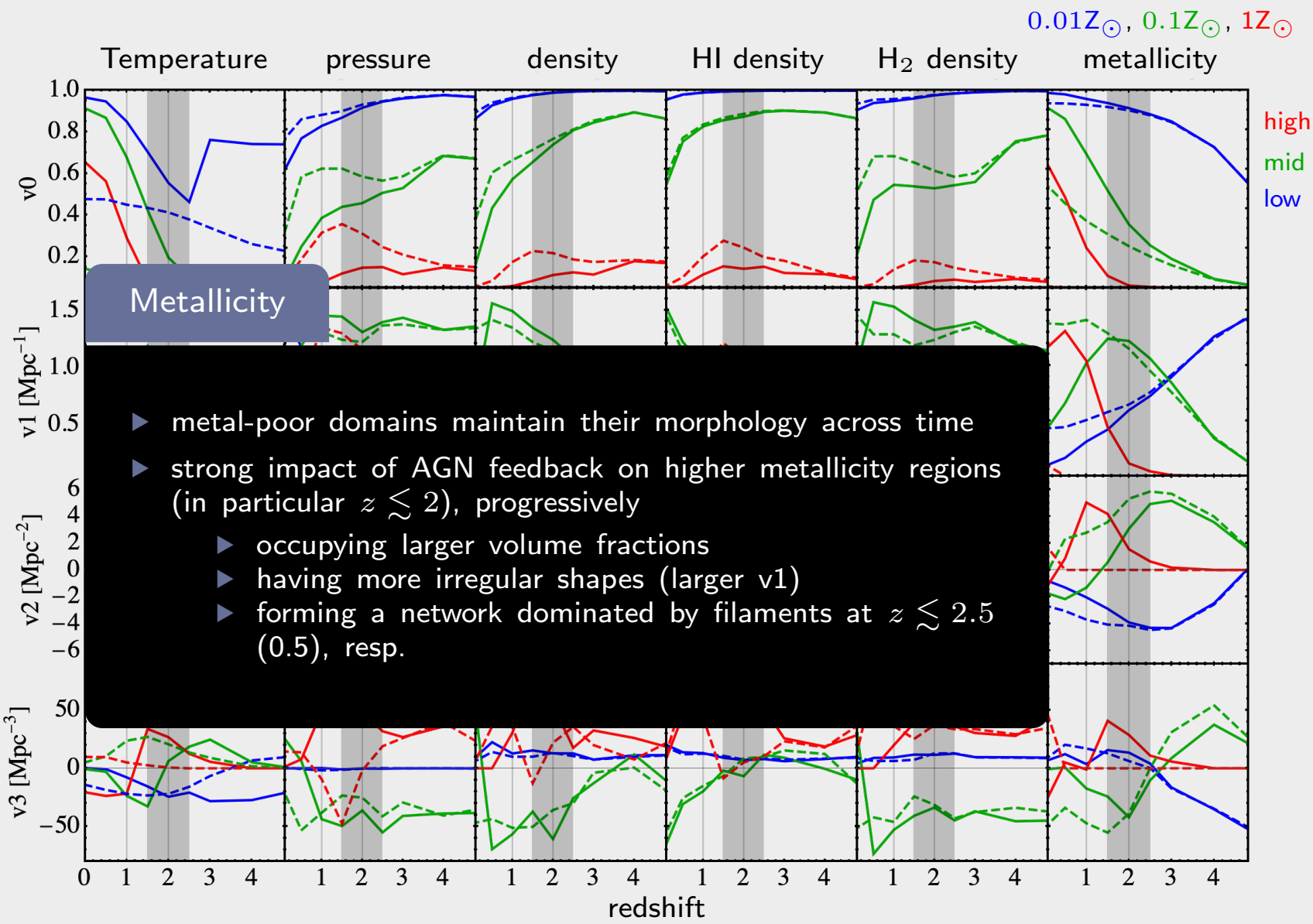


Metallicity

- metal-poor domains maintain their morphology across time
- strong impact of AGN feedback on higher metallicity regions (in particular $z \lesssim 2$), progressively
  - occupying larger volume fractions
  - having more irregular shapes (larger v1)

Time evolution of MFs

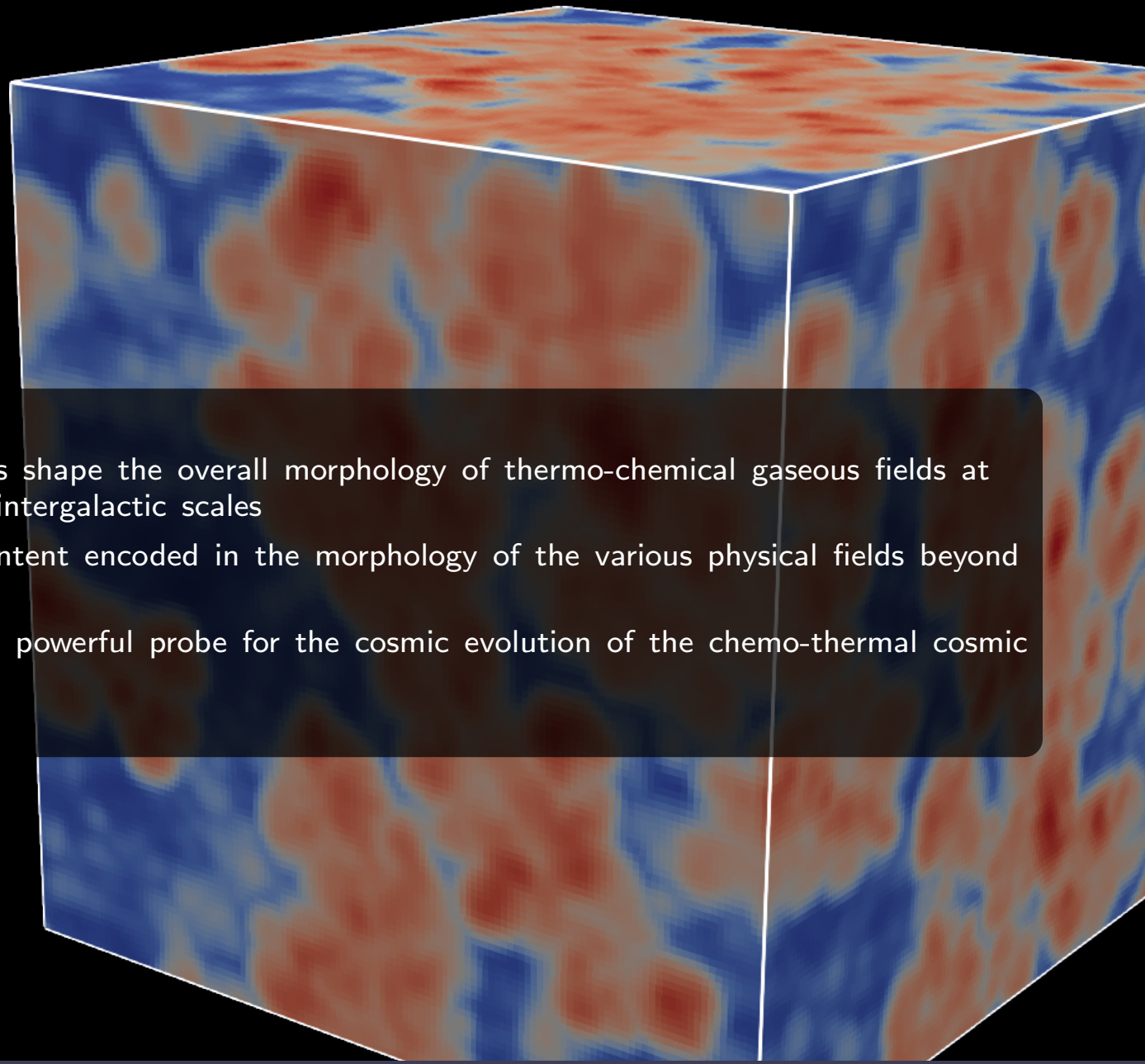
Fiducial: AGN & stellar feedback
noAGN: stellar feedback



Metallicity

- metal-poor domains maintain their morphology across time
- strong impact of AGN feedback on higher metallicity regions (in particular $z \lesssim 2$), progressively
  - occupying larger volume fractions
  - having more irregular shapes (larger v1)
  - forming a network dominated by filaments at $z \lesssim 2.5$ (0.5), resp.

Baryons on large scales



Morphology

- small-scale processes shape the overall morphology of thermo-chemical gaseous fields at circumgalactic and intergalactic scales
- high information content encoded in the morphology of the various physical fields beyond the total density
- highlights MFs as a powerful probe for the cosmic evolution of the chemo-thermal cosmic web

Koendrink invariants

- random field $\nu(\mathbf{x})$ on a d-dimensional support $\mathcal{D} \subseteq \mathbb{R}^d$

  $\rightarrow F_\nu$ - excursion set for a given threshold ν

$$F_\nu = \{\mathbf{x} \in \mathcal{D} | \nu(\mathbf{x}) \geq \nu\}$$

Koendrink invariants

- random field $\nu(\mathbf{x})$ on a d-dimensional support $\mathcal{D} \subseteq \mathbb{R}^d$

  $\rightarrow$ F_ν - excursion set for a given threshold ν

  $$F_\nu = \{\mathbf{x} \in \mathcal{D} | \nu(\mathbf{x}) \geq \nu\}$$

  $\rightarrow$ Minkowski functionals (per unit volume) for $d = 3$:

  $$v_0(\nu) = \frac{1}{|\mathcal{D}|} \int_{\mathcal{D}} d^3x \, \Theta\left[\nu - \nu(\mathbf{x})\right]$$

  $$v_k(\nu) = \frac{1}{|\mathcal{D}|} \int_{\partial F_\nu} d^2A(\mathbf{x}) \, v_k^{(\mathrm{loc})}(\nu, \mathbf{x})$$

  with
  $$v_1^{(\mathrm{loc})}(\nu, \mathbf{x}) = \frac{1}{6}$$
  $$v_2^{(\mathrm{loc})}(\nu, \mathbf{x}) = \frac{1}{6\pi} \left(\frac{1}{R_1(\mathbf{x})} + \frac{1}{R_2(\mathbf{x})} \right)$$
  $$v_3^{(\mathrm{loc})}(\nu, \mathbf{x}) = \frac{1}{4\pi} \frac{1}{R_1(\mathbf{x}) R_2(\mathbf{x})}$$

Koendrink invariants

- random field $\nu(\mathbf{x})$ on a d-dimensional support $\mathcal{D} \subseteq \mathbb{R}^d$

  $\rightarrow F_\nu$ - excursion set for a given threshold ν

  $$F_\nu = \{\mathbf{x} \in \mathcal{D} | \nu(\mathbf{x}) \geq \nu\}$$

  $\rightarrow$ Minkowski functionals (per unit volume) for $d = 3$:

  $$v_0(\nu) = \frac{1}{|\mathcal{D}|} \int_{\mathcal{D}} d^3x \, \Theta\left[\nu - \nu(\mathbf{x})\right]$$

  $$v_k(\nu) = \frac{1}{|\mathcal{D}|} \int_{\partial F_\nu} d^2A(\mathbf{x}) \, v_k^{(\mathrm{loc})}(\nu, \mathbf{x})$$

  with
  $$v_1^{(\mathrm{loc})}(\nu, \mathbf{x}) = \frac{1}{6}$$
  $$v_2^{(\mathrm{loc})}(\nu, \mathbf{x}) = \frac{1}{6\pi} \left(\frac{1}{R_1(\mathbf{x})} + \frac{1}{R_2(\mathbf{x})} \right)$$
  $$v_3^{(\mathrm{loc})}(\nu, \mathbf{x}) = \frac{1}{4\pi} \frac{1}{R_1(\mathbf{x}) R_2(\mathbf{x})}$$

- transform the surface integrals into volume integrals:

  $$v_k(\nu) = \frac{1}{|\mathcal{D}|} \int_{\mathcal{D}} d^3x \, \delta\left[\nu - \nu(\mathbf{x})\right] |\nabla \nu(\mathbf{x})| v_k^{(\mathrm{loc})}(\nu, \mathbf{x})$$

  with $v_k^{(\mathrm{loc})}(\nu, \mathbf{x})$ - in terms of Koendrink invariants (Konedrink 1984) formed from the 1st and 2nd derivatives of the field (e.g. Schmalzing & Buchert 1997)

Koendrink invariants

- density field $u(\mathbf{x})$ sampled at the grid points of a cubic lattice

  $\rightarrow$ F_ν - excursion set for a given threshold ν

$$F_\nu = \{\mathbf{x} \in \mathcal{D} | u(\mathbf{x}) \geq \nu\}$$

  $\rightarrow$ Minkowski functionals (per unit volume):

$$\hat{v}_0(\nu) = \frac{1}{|\mathcal{D}|} \int_{\mathcal{D}} d^3x \, \Theta\left[u - \nu\right]$$

$$\hat{v}_1(\nu) = \frac{1}{|\mathcal{D}|} \int_{\mathcal{D}} d^3x \, \frac{1}{6} \delta(u - \nu) (u_{,i} u_{,i})^{1/2}$$

$$\hat{v}_2(\nu) = \frac{1}{|\mathcal{D}|} \int_{\mathcal{D}} d^3x \, \frac{1}{3\pi} \delta(u - \nu) \frac{\epsilon_{ijm} \epsilon_{klm} u_{,i} u_{,jk} u_{,l}}{2 u_{,n} u_{,n}}$$

$$\hat{v}_3(\nu) = \frac{1}{|\mathcal{D}|} \int_{\mathcal{D}} d^3x \, \frac{1}{4\pi} \delta(u - \nu) \frac{\epsilon_{ijk} \epsilon_{lmn} u_{,i} u_{,l} u_{,jm} u_{,kn}}{2 (u_{,p} u_{,p})^{3/2}}$$

with $u_{,i}$, $u_{,ij}$ 1st and 2nd field's derivatives